ANNALS OF CARNEGIE MUSEUM

VOL. 86, NUMBER 1, PP. 1–35 31 MARCH 2020

ANATOMY OF THE PETROSAL AND MIDDLE EAR OF THE BROWN RAT, *RATTUS NORVEGICUS* (BERKENHOUT, 1769) (RODENTIA, MURIDAE)

JOHN R. WIBLE
Curator, Section of Mammals, Carnegie Museum of Natural History
5800 Baum Boulevard, Pittsburgh, Pennsylvania 15206

SARAH L. SHELLEY
Postdoctoral Fellow, Section of Mammals, Carnegie Museum of Natural History
5800 Baum Boulevard, Pittsburgh, Pennsylvania 15206

ABSTRACT

The anatomy of the petrosal and associated middle ear structures are described and illustrated for the brown rat, *Rattus norvegicus* (Berkenhout, 1769). Although the middle ear in this iconic mammal has been treated by prior authors, there has not been a comprehensive, well-illustrated contribution using current anatomical terminology. Descriptions are based on specimens from the osteological collections of the Section of Mammals, Carnegie Museum of Natural History, and a CT scanned osteological specimen from the Texas Memorial Museum. The petrosal, ectotympanic, malleus, incus, stapes, and inner ear were segmented from the CT scans.

The petrosal of the brown rat is only loosely attached to the cranium, primarily along its posterior border; it is separated from the basisphenoid, alisphenoid, and squamosal by a large piriform fenestra that transmits various neurovascular structures including the postglenoid vein. The extent of the piriform fenestra broadly exposes the tegmen tympani of the petrosal in lateral view. The floor of the middle ear is formed by the expanded ectotympanic bulla, which is tightly held to the petrosal with five points of contact. The surfaces of the petrosal affording contact with the ectotympanic bulla are the rostral tympanic process, the epitympanic wing, the tegmen tympani, two of the three parts of the caudal tympanic process, and the tympanohyal, with the ectotympanic fused to the last. The ectotympanic in turn is fused to the elongate rostral process of the malleus, which is only discoverable through the study of juvenile specimens. In addition to osteology, the major nerves, arteries, and veins of the petrosal are described and illustrated based on the literature and osteological correlates.

The petrosal of the brown rat is compared with those of several Eocene rodents to put the extant form in the context of early members of the rodent lineage. Comparisons benefitted from CT scans of the middle Eocene ischromyoid *Paramys delicatus* Leidy, 1871, from the western United States, affording the first description of the endocranial surface of the petrosal in an Eocene rodent. The petrosals in the Eocene fossils are more tightly held in the cranium, but the ectotympanic contacts the petrosal through the same five points, with some modifications. The most unexpected discovery in *Paramys delicatus* was the presence of a prominent tentorial process of the parietal in contact with the reduced crista petrosa.

KEY WORDS: basicranium, brown rat, Eocene, middle ear anatomy, *Paramys delicatus*, petrosal

INTRODUCTION

Discoveries of Mesozoic fossils preserving the petrosal and/or auditory ossicles are occurring at a rapid pace, which has made the evolution of the middle ear apparatus in the mammal lineage one of the best documented and oft cited examples of a morphological transformation series in vertebrates (Luo 2011). In addition to informing evolutionary models of transformational change, these bony elements are important sources of characters for phylogenetic analysis across Mammaliaformes, the broader clade of mammals and their extinct relatives. The study of ontogeny and adult morphology of extant mammals is critical for providing the bases for transformational models and for proposing hypotheses of homology across the component parts. Toward that end, over the last few years, the senior author has been reporting on the petrosal and osseous middle ear elements in various extant mammals (e.g., Wible 2009, 2010, 2011, 2012). The current report follows in this mode by describing these structures in an iconic extant placental, the brown rat, *Rattus norvegicus* (Berkenhout, 1769), also known as the common rat, domestic rat, fancy rat, lab rat, Norway rat, or sewer rat (Burgin 2017).

Rodents are the most diverse clade of extant mammals accounting for 2,552 of 6,111 species of placentals recognized by Burgin et al. (2018). Muridae, the family including *R. norvegicus*, is the most diverse within Rodentia, with 834 species (Burgin et al. 2018). Sixty-six species of *Rattus* Fischer, 1803, are recognized by Musser and Carleton (2005). From proposed origins in central Asia, *R. norvegicus* has spread in company with humans to all continents except Antarctica and is the stock from which the common laboratory rat was derived (Lindsey and Baker 2006). Given its preeminent role in biomedical research, the brown rat has been the subject of numerous contributions regarding all aspects of its anatomy. The most comprehensive anatomical treatments are those of Greene (1935), Hebel and Stromberg (1976), Popesko et al. (1992), and Maynard and Downes (2019), although their treatments of the skull are not in much detail. A vast literature addressing rat middle ear anatomy already exists, including general overviews (e.g., Hellström et al. 1982; Judkins and Li 1997), on osteology (e.g., Parent 1980, 1983; Wysocki 2008), on vasculature (e.g., Tandler 1899; Nabeya 1923; Guthrie 1963; Szabó 1990, 1995), on musculature (e.g., Berge and Wirtz 1989; Berge and Wal 1990), and on aspects of development (e.g., Youssef 1966, 1969). Yet, there is not a well-illustrated comprehensive treatment on the petrosal osteology in the

current comparative anatomical language. It is the goal of this report to fill that void. However, it is not a goal here to compare the middle ear of the brown rat broadly across Placentalia, Euarchontoglires, or Rodentia. Our comparisons are limited to some early and middle Eocene rodents in order to place the brown rat in context with the early members of the rodent lineage.

MATERIALS AND METHODS

Extant osteological specimens studied with a stereomicroscope are from the Section of Mammals, Carnegie Museum of Natural History (CM). Adults are those with fully erupted M1–3. The primary specimens referred to in the text are:

Rattus norvegicus, CM 493, juvenile male, Pittsburgh, Pennsylvania, U.S.A., October, 1898. M3 is in the process of erupting.

Rattus norvegicus, CM 10227, adult female, Butler County, Pennsylvania, U.S.A., October 25, 1934.

Rattus norvegicus, CM 17504, adult female, Pittsburgh, Allegheny County, Pennsylvania, U.S.A., July 14, 1939.

Rattus norvegicus, CM 18604, young adult female, Andover, Essex County, Massachusetts, U.S.A., June 10, 1933. All molars are erupted but sutures between the components of the occipital bone are retained (basi-, ex-, and supraoccipital).

Rattus norvegicus, CM 21415, juvenile male, Dormont, Allegheny County, Pennsylvania, U.S.A., April 29, 1943. M3 is in the process of erupting.

Rattus norvegicus, CM 29584, adult male, Somerset, Somerset County, Pennsylvania, U.S.A., August 8, 1949.

Rattus norvegicus, CM Teaching Collection, adult of unknown sex and geographic origin. Only the skull is known. There is no accompanying data, although its identification to species was confirmed by the late Guy Musser, Curator Emeritus, American Museum of Natural History. Because of the lack of data, we forcedly detached the auditory bulla from the petrosal and then the petrosal from the cranium.

Rattus rattus, CM 101347, juvenile male, Exu, State of Pernambuco, Brazil, April 15, 1977. M3 is fully formed and in a crypt.

In addition, two micro-CT datasets were studied:

Rattus norvegicus, Texas Memorial Museum M-2272, West Point, Hancock County, Illinois, U.S.A. Data were downloaded from DigiMorph.org (http://digimorph.org/specimens/Rattus_norvegicus/); University of Texas High-Resolution X-ray CT Facility Archive 2660, scanning funded by Ms. Jeri Rodgers. The specimen was scanned January 20, 2012 along the coronal axis for a total of 1571 slices, each 1024 x 1024 slice being 0.02961 mm, with interslice spacing of 0.02961 mm and a field of reconstruction of 28 mm. The right petrosal, ectotympanic, malleus, incus, stapes, and inner ear were segmented in Avizo 9.5.0 software (Visualization and Sciences Group, 1995–2018).

Paramys delicatus, American Museum of Natural History (AMNH-FM) 12506, Black Fork Member, middle Eocene, Bridger Formation, Bridger Basin, Wyoming, USA. Data were downloaded from morphosource.org (https://www.morphosource.org/Detail/SpecimenDetail/Show/specimen_id/2381) with the permission of the AMNH. Details on this scan are included in the supplemental material to Bertrand et al. (2016). The left petrosal was segmented in Avizo 9.5.0 software (Visualization and Sciences Group, 1995–2018).

The anatomical terminology employed follows that in prior publications by the senior author (e.g., Wible 2008, 2009, 2010, 2011, 2012). Usage of English equivalents of the Nomina Anatomica Veterinaria (Fifth Edition, 2005), abbreviated NAV here, is preferred when appropriate. For certain anatomical systems, the NAV is not adequate because its comparative base is not sufficiently broad. In particular, this is the case for the vasculature and for the ectotympanic and middle-ear ossicles. For the former, we employ the terminology in Wible (1984, 1987), and for the latter in Henson (1961).

Institutional Abbreviations

AMNH—Department of Vertebrate Paleontology, American Museum of Natural History, New York, New York, U.S.A.

CM—Section of Mammals, Carnegie Museum of Natural History, Pittsburgh, Pennsylvania, U.S.A.

TMM—Texas Memorial Museum, University of Texas, Austin, Texas, U.S.A.

USNM—National Museum of Natural History, Smithsonian Institution, Washington, D.C., U.S.A.

DESCRIPTIONS

Overview

In ventral view in situ in the brown rat cranium, most of the petrosal is hidden by the auditory bulla, which is formed by the expanded ectotympanic bone (“e” in Fig. 1). Small portions of the petrosal are exposed ventrally posteromedial and posterolateral to the bulla. The medial margin of the petrosal approximates the occipital bone, here composed of the fused basi- and exoccipital (“bo” and “eo,” respectively in Fig. 1). The petrosal and basioccipital (based on CM 18604, a juvenile preserving sutures within the occipital bone) contact in some specimens (e.g., CM 17504) but in others (e.g., CM 10227) are separated by a gap, the basicapsular fissure or fenestra (De Beer 1937; petrobasilar fissure of Popesko et al. 1992). The contact occurs along the raised lateral lip of the basioccipital, which represents a tympanic process of that bone (“tpbo” in Fig. 1). At the anterior and posterior ends of the petrosal’s medial margin with the occipital are two neurovascular conduits, the carotid canal and the jugular foramen, respectively. The

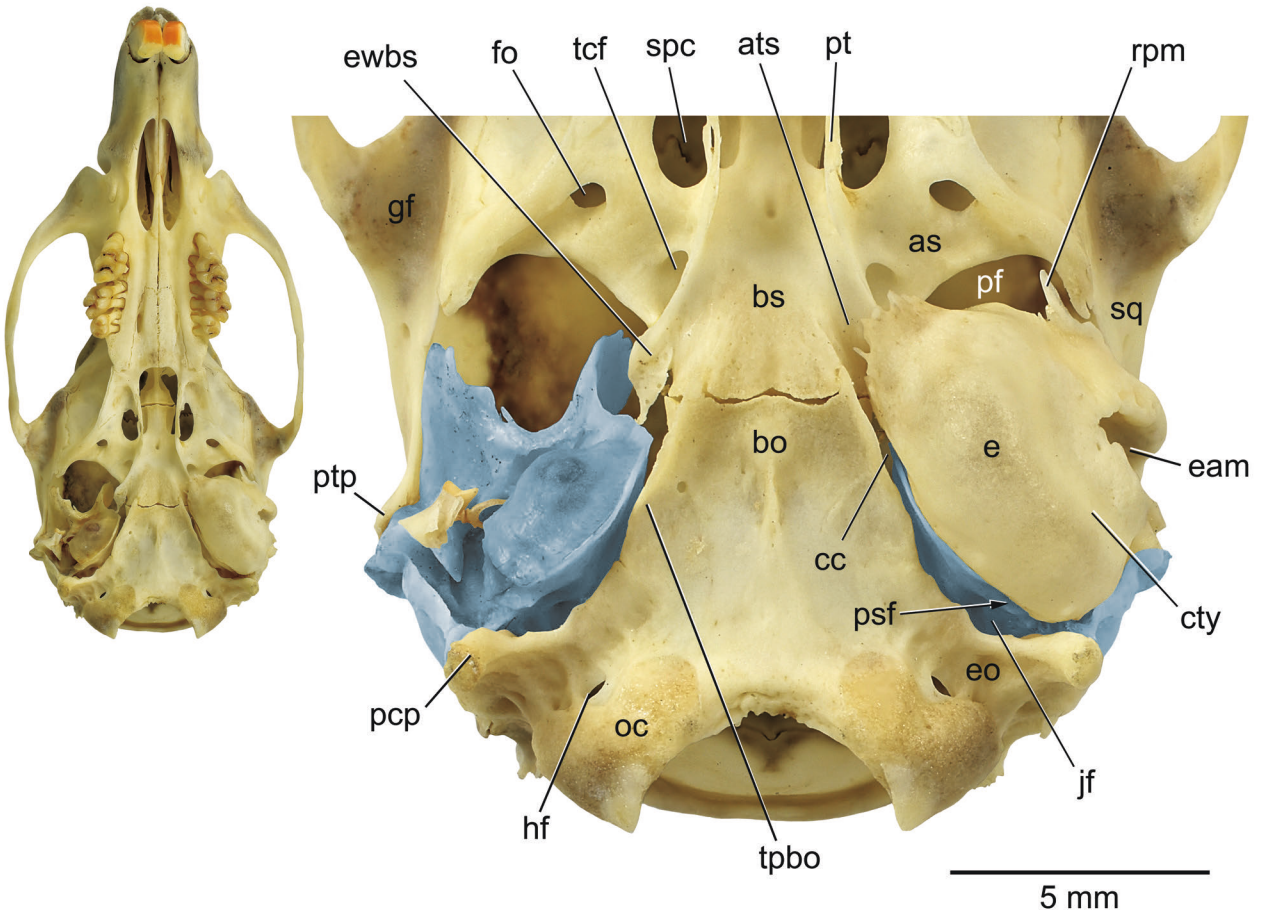

Fig. 1.—*Rattus norvegicus*, CM 10227, cranium in ventral view with enlarged basicranium. The left and right petrosals are in light blue; the right ectotympanic and malleus are removed, except for a small remnant of the posterior crus of the ectotympanic lying ventral to the incus and stapes. Abbreviations: **as,** alisphenoid; **ats,** auditory tube sulcus; **bo,** basioccipital; **bs,** basisphenoid; **cc,** carotid canal; **cty,** crista tympanica; **e,** ectotympanic; **eam,** external acoustic meatus; **eo,** exoccipital; **ewbs,** epitympanic wing of basisphenoid; **fo,** foramen ovale; **gf,** glenoid fossa; **hf,** hypoglossal foramen; **jf,** jugular foramen; **oc,** occipital condyle; **pcp,** paracondylar process of exoccipital; **pf,** piriform fenestra; **psf,** proximal stapedial artery foramen; **pt,** pterygoid; **ptp,** posttympanic process of squamosal; **rpm,** rostral process of malleus; **spc,** sphenopterygoid canal; **sq,** squamosal; **tcf,** transverse canal foramen; **tpbo,** tympanic process of basioccipital.

carotid canal ("cc" in Fig. 1) for the internal carotid artery and nerve (Greene 1935; Wible 1984) is more a gap between the ectotympanic, petrosal, and basioccipital than an enclosed canal. The jugular foramen ("jf" in Fig. 1; posterior lacerated foramen of Greene 1935) for the internal jugular vein along with cranial nerves IX, X, and XI (Greene 1935) is between the petrosal and exoccipital (based on CM 18604). Ventrolateral to the jugular foramen and hidden in direct ventral view is the proximal stapedial foramen ("psf" in Fig. 1) between the petrosal and ectotympanic transmitting a branch of the internal carotid, the stapedial artery (pterygopalatine artery of Greene 1935), into the middle ear. For descriptive purposes, we divide the stapedial artery into proximal and distal parts by their relationship to the stapes and apply those positional descriptors to the corresponding grooves and foramina for the vessel's subdivisions.

The rear of the petrosal is wedged between the exoccipital medially and the squamosal laterally. Where the petrosal abuts the exoccipital, the latter has a prominent muscular process, the paracondylar process ("pcp" in Fig. 1; paramastoid process of Greene 1935; paroccipital process of Wahlert 1974), which provides attachment for the sternomastoid and digastric muscles (Greene 1935). Where the petrosal abuts the squamosal, the latter has a very weak posttympanic process ("ptp" in Fig. 1; occipital process of Popesko et al. 1992; post-tympanic hook of Maynard and Downes 2019), which lies entirely dorsal to the external acoustic meatus, best seen in lateral view (Fig. 2). Hidden in the interval between these two processes is the stylomastoid foramen between the petrosal and ectotympanic ("smf" in Fig. 2), which transmits the facial nerve, cranial nerve VII, from the middle ear (Greene 1935).

Anterior and anterolateral to the petrosal is a large

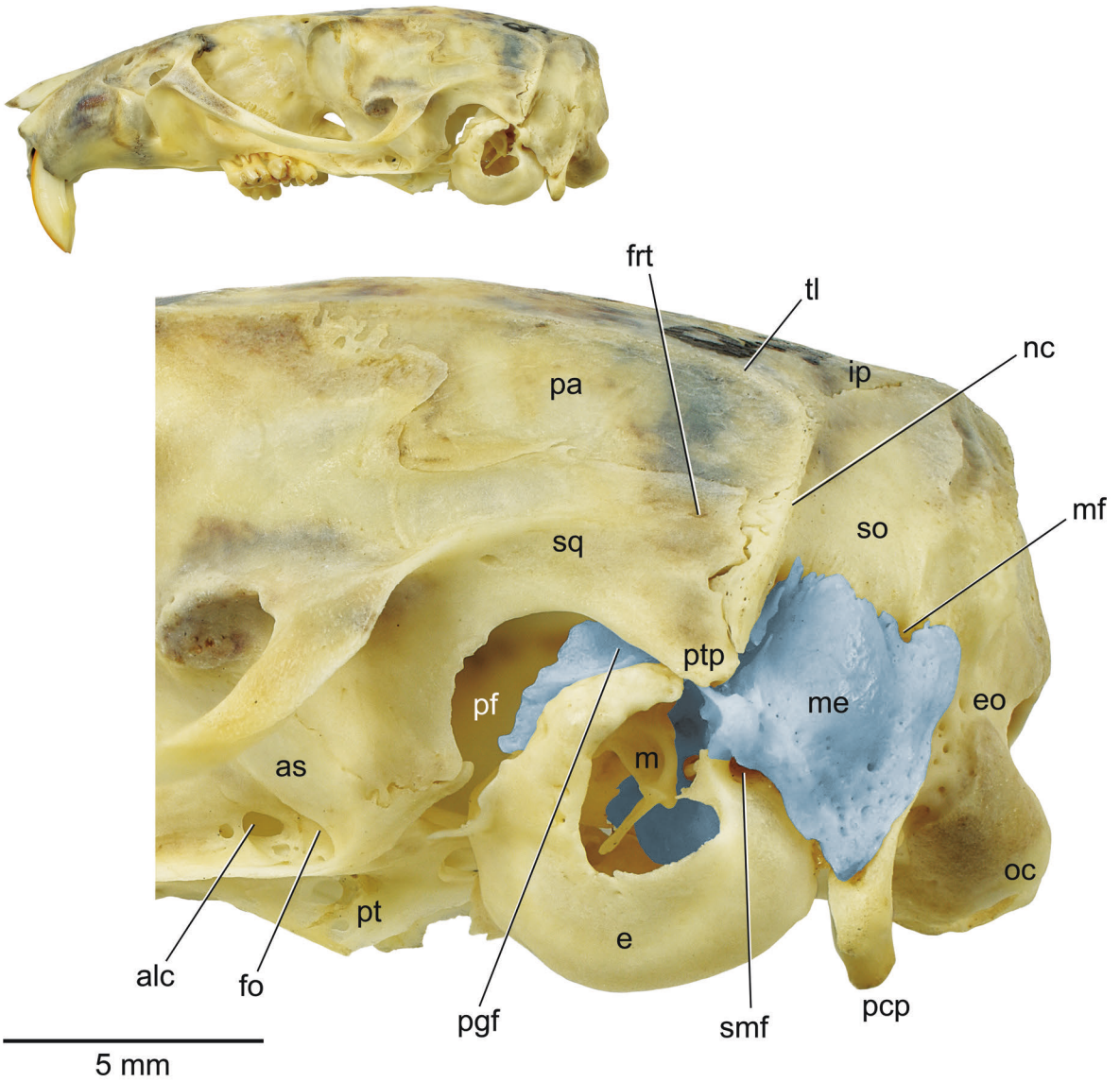

Fig. 2.—*Rattus norvegicus*, CM 10227, cranium in left lateral view. Left petrosal is in light blue; the left incus is missing. Abbreviations: **alc,** alisphenoid canal; **as,** alisphenoid; **e,** ectotympanic; **eo,** exoccipital; **fo,** foramen ovale; **frt,** foramen for ramus temporalis; **ip,** interparietal; **m,** malleus; **me,** mastoid exposure; **mf,** mastoid foramen; **nc,** nuchal crest; **oc,** occipital condyle; **pa,** parietal; **pcp,** paracondylar process of exoccipital; **pf,** piriform fenestra; **pgf,** postglenoid foramen; **pt,** pterygoid; **ptp,** posttympanic process of squamosal; **smf,** stylomastoid foramen; **so,** supraoccipital; **sq,** squamosal; **tl,** temporal line.

opening formed by two crescent-shaped, confluent gaps separating the petrosal and bulla from the alisphenoid and squamosal ("pf" in Figs. 1–2). This wide gap is the piriform fenestra (pyriform fenestra of McDowell 1958; middle lacerate foramen of Wahlert 1974; petrotympanic fissure of Popesko et al. 1992), which as documented here transmits several neurovascular structures. At the anteromedial corner of the bulla is a large opening into the middle ear hidden by the ectotympanic in direct ventral view. This opening, the musculotubal canal (Eustachian canal), is for the auditory tube (pharyngotympanic or Eustachian tube); it lies between the ectotympanic, petrosal, and basisphenoid, and directs this connection between the middle ear and nasopharynx into a broad, anteromedially directed sulcus on the basisphenoid ("ats" in Fig. 1).

In lateral view in situ in the cranium, the petrosal has a broad quadrangular contribution to the posteroventral braincase wall, the mastoid exposure ("me" in Fig. 2). The anterior, dorsal, and posterior sides of the quadrangle abut the occipital bone. Based on the juvenile CM 18604, the

exoccipital contacts the posterior side of the quadrangle and the supraoccipital the dorsal and anterior sides ("so" in Fig. 2) with a small area of contact with the posttympanic process of the squamosal anteroventrally. In the dorsal suture with the supraoccipital is a small mastoid foramen ("mf" in Fig. 2) transmitting a vein to the sigmoid sinus (Butler 1967). The ventral margin of the mastoid exposure is free, separated on its anterior surface from the ectotympanic by a narrow gap. It is in the anterior end of this gap that the stylomastoid foramen is situated ("smf" in Fig. 2). Anterior to the mastoid exposure, a sliver of the petrosal is visible in the interval deep to the squamosal and ectotympanic, anterodorsal to the external acoustic meatus, in the posterolateral aspect of the piriform fenestra. In the rear of this interval between the petrosal and squamosal is the exit for the postglenoid vein (transverse sinus of Greene 1935; retroglenoid vein of Popesko et al. 1992) from the cranial cavity (Hill 1935; "pgf" in Fig. 2). This opening represents a postglenoid foramen that is not fully enclosed in bone.

In endocranial view in situ in the cranium, based on the CT scans of TTM M-2247, the petrosal is broadly exposed in the caudal cranial fossa and appears to have a smaller exposure in the middle cranial fossa ("ccf" and "mcf," respectively in Fig. 3). However, the pronounced crista petrosa ("crp" in Fig. 3) marking the boundary of these two endocranial spaces hides most of the petrosal's contribution to the middle cranial fossa in direct medial view. The petrosal is positioned on top of the ectotympanic, which has a small exposure in the floor of these two cranial fossae. The petrosal contacts the squamosal and supraoccipital dorsally and the exoccipital posteriorly. As noted above, the petrosal approximates the basioccipital medially and is separated from the alisphenoid and squamosal anteriorly by the piriform fenestra.

Petrosal

In extant therian mammals, the petrosal is a paired endochondral bone enclosing the inner ear and contributing to the roof of the middle ear. Following Wible (1990), we describe the petrosal in two parts: the pars cochlearis ("pco" in Fig. 4A), enclosing the cochlea ("co" in Fig. 4C) and saccule, and the pars canalicularis ("pca" in Fig. 4A), enclosing the utricle and semicircular canals (Figs. 4B–C). A large subdivision of the pars canalicularis is the tegmen tympani ("tt" in Fig. 4A), which forms a roof over the malleus and incus. This subdivision between the pars cochlearis and pars canalicularis is equivalent to the petrous and mastoid parts of other authors (e.g., MacIntyre 1972). A definitive boundary delimiting the two parts does not exist: the pars cochlearis and pars canalicularis are generally positioned anteroventromedially and posterodorsolaterally, respectively.

During ontogeny a variety of processes grow from the core cartilaginous capsule of the chondrocranium that encloses the inner ear (gray in Fig. 5A). Based on his developmental studies in primates, treeshrews, elephant shrews, and lipotyphlans, MacPhee (1981) identified two classes of such processes, which generally have been followed by subsequent researchers: tympanic processes in the middle ear floor (blue and purple in Fig. 5A) and epitympanic wings in the middle ear roof (red in Fig. 5A). Although we are only considering these processes on the petrosal here, MacPhee (1981) used the same terminology to describe processes into the tympanic floor and roof from bones neighboring the petrosal (i.e., alisphenoid, basisphenoid, basioccipital, exoccipital, and squamosal). Tympanic processes grow into a plane of connective tissue stretched between the primordial petrosal and the ectotympanic bone, which MacPhee (1981) called the fibrous membrane of the tympanic cavity; epitympanic wings grow into a plane of connective tissue that covers the piriform fenestra, the gap anterior to the primordial petrosal that separates it from the squamosal, alisphenoid, and basisphenoid. Regarding the petrosal epitympanic wing, it grows from the anterior aspect of the pars cochlearis (red in Fig. 5A). Regarding the petrosal tympanic processes, MacPhee (1981) recognized two sorts: a rostral tympanic process derived from the pars cochlearis (blue in Fig. 5A) and a caudal tympanic process from the pars canalicularis (purple in Fig. 5A). For the caudal tympanic process, he recognized three parts: a medial section ("1" in Fig. 5A) and two lateral sections distinguished by their positional relationship to the origin of the stapedius muscle ("*" in Fig. 5A), that is, a lateral section medial to the stapedius muscle ("2" in Fig. 5A) and a lateral section lateral to the stapedius muscle ("3" in Fig. 5A). The epitympanic wing and rostral and caudal tympanic processes have become rich sources of characters for phylogenetic analysis regarding their presence, size, and contribution to neurovascular passageways.

In Figure 5B, we apply MacPhee's (1981) schema to the petrosal of the adult brown rat to illustrate the basis for our terminology of outgrowths to the pars cochlearis and pars canalicularis. At first glance, the petrosal of the adult brown rat may seem complicated. However, this complexity fits well into MacPhee's (1981) schema with the rat petrosal having an expanded epitympanic wing and a full complement of rostral and caudal tympanic processes. Obvious differences between MacPhee's schema and the adult brown rat concern the lack of connection between the rostral and caudal tympanic processes as well as between the two lateral sections of the caudal tympanic process ("2" and "3" in Fig. 5B).

Ventral view.—The pars cochlearis of the brown rat is dominated by a roughly ovoid promontorium, longer than wide with the long axis directed anteromedially in the intact cranium ("pr" in Fig. 6A; see also Fig. 1). The promontorium encloses the coils of the cochlea (Fig. 4). Burda et al. (1988) reported 2.2 coils for *R. norvegicus* (2.5 in Nabeya 1923; Albuquerque et al. 2009); in the CT scanned specimen studied here, following the method of Ekdale (2013), the left cochlear duct coils 790° equivalent to 2.2 coils (Fig. 4C). In the cranium, the ventral limit of

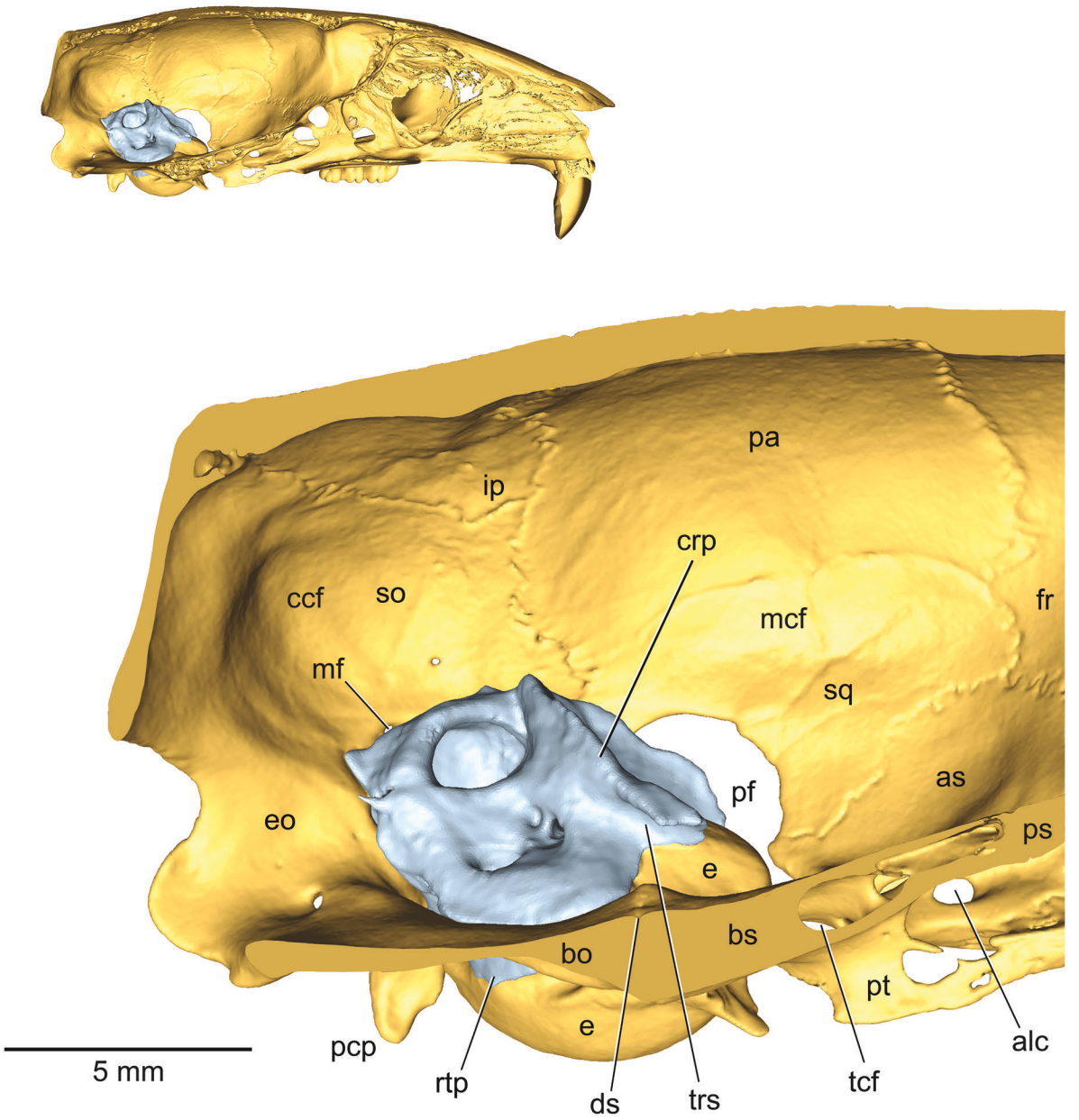

Fig. 3.—*Rattus norvegicus*, TMM M-2272, mid-sagittal ortho slice of isosurface rendered from CT data. Petrosal is in light blue; for simplification, the spongy bone along the cut midline edge has been filled in with uniform color and only the major midline vascular conduits have been left open. Abbreviations: **alc,** alisphenoid canal; **as,** alisphenoid; **bo,** basioccipital; **bs,** basisphenoid; **ccf,** caudal cranial fossa; **crp,** crista petrosa; **ds,** dorsum sellae; **e,** ectotympanic; **eo,** exoccipital; **fr,** frontal; **ip,** interparietal; **mcf,** middle cranial fossa; **mf,** mastoid foramen; **pa,** parietal; **pcp,** paracondylar process of exoccipital; **pf,** piriform fenestra; **ps,** presphenoid; **pt,** pterygoid; **rtp,** rostral tympanic process of petrosal; **so,** supraoccipital; **sq,** squamosal; **tcf,** transverse canal foramen; **trs,** trigeminal sulcus.

the promontorium is roughly in the same plane as the tympanic process of the basioccipital (Fig. 1).

Extending medially, anteriorly, and anterolaterally from the promontorium is a continuous bony shelf. We identify the thin, flange-like, medial part of this shelf as the rostral tympanic process (blue in Fig. 5B; "rtp" in Fig. 6A), because it is angled obliquely such that it approaches or contacts the tympanic process of the basioccipital (Fig. 1) and it broadly contacts the ectotympanic bulla ("1" in Fig. 6B). The anterior and anterolateral part of this shelf, the epitympanic wing (red in Fig. 5B; "ew" in Fig. 6A), is in a nearly horizontal plane. The rostral tympanic pro-

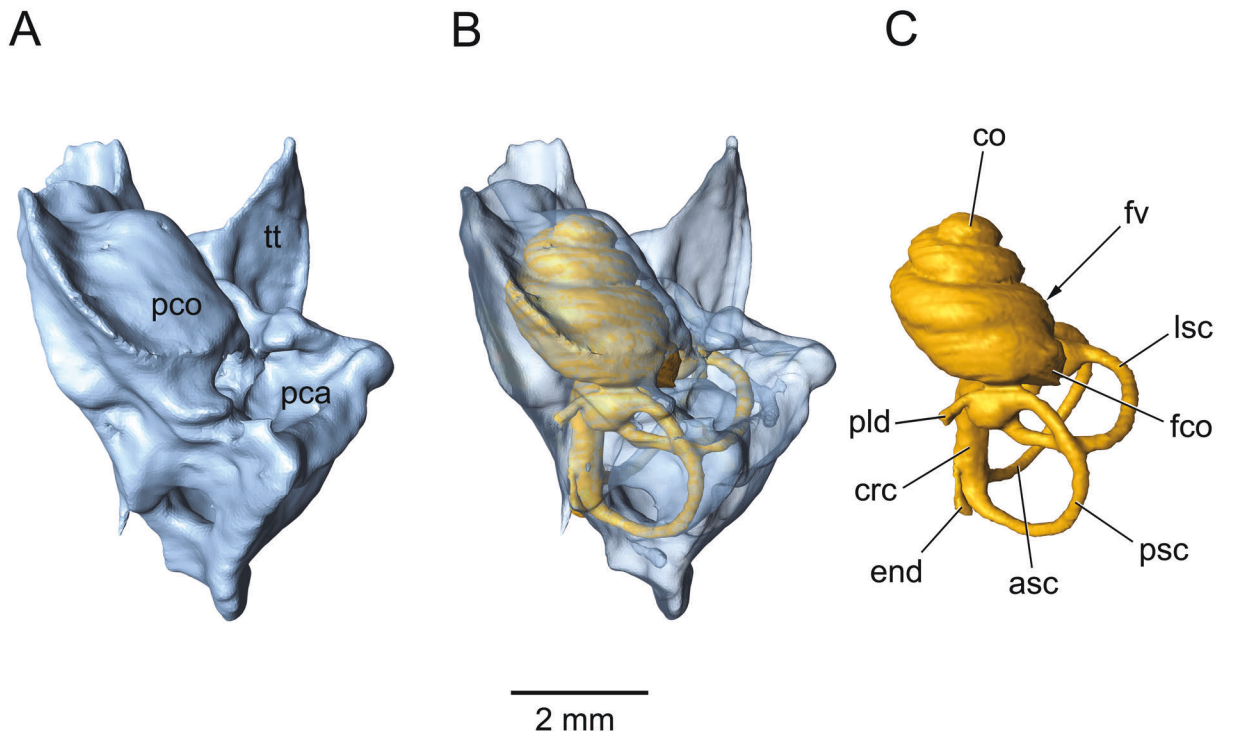

Fig. 4.—*Rattus norvegicus*, TMM M-2272, isosurface rendered from CT data of left petrosal and inner ear in ventral view as positioned in the cranium, anterior to the top of the page. **A,** petrosal; **B,** transparent petrosal (light blue) showing inner ear (gold); **C,** inner ear. Abbreviations: **asc,** anterior semicircular canal; **co,** cochlea; **crc,** crus commune; **end,** endolymphatic duct; **fco,** fenestra cochleae; **fv,** fenestra vestibuli; **lsc,** lateral semicircular canal; **pca,** pars canalicularis; **pco,** pars cochlearis; **pld,** perilymphatic duct; **psc,** posterior semicircular canal; **tt,** tegmen tympani.

cess and epitympanic wing are partially separated by a low septum extending anteriorly from the promontorium. The epitympanic wing is wider than the promontorium and divided into medial and lateral sections by a low oblique ridge. The medial section is a deep concavity, longer than wide, serving as the origin for the tensor tympani muscle (Berge and Wirtz 1989a; "ttf" in Fig. 6A). The lateral section is a shallow concavity, also longer than wide, that provides attachment for the ectotympanic bulla ("2" in Fig. 6B). The anterolateral part of the epitympanic wing has a small, slit-like aperture leading into a narrow, anteromedially directed groove; this is the hiatus Fallopii ("hF" in Fig. 6A) for the greater petrosal nerve (Berge and Wirtz 1989a; Berge and Wal 1990; "gpn" in Fig. 6C). The position of the hiatus varies with respect to the oblique ridge between the medial and lateral sections of the epitympanic wing: it is lateral to the ridge in some (as illustrated in Fig. 6; e.g., CM 17504) and medial in others (e.g., CM 10227).

A large, oval aperture, wider than high, penetrates the posterior aspect of the pars cochlearis ("acf" in Fig. 6A). Recessed within this aperture, and hidden in ventral view, is a thin ridge representing the point of attachment for the secondary tympanic membrane, which marks the location of the round window or fenestra cochleae (Hellström et al. 1988). The aperture in the surface of the pars cochlearis leading to the fenestra cochleae is the aperture of the cochlear fossula (sensu MacPhee 1981). In the intact cranium, the aperture points posterolaterally (Fig. 1). Posterior to the aperture of the cochlear fossula is a low, rounded, curved ridge on the pars canalicularis, which forms the posterior wall of a recess, the cochlear fossula ("cf" in Fig. 6A). Following MacPhee (1981), we identify this ridge as part of the caudal tympanic process ("1" and "2" on purple in Fig. 5B; "ctp1&2" in Fig. 6A). A well-developed groove for the proximal stapedial artery crosses the posterior aspect of the pars cochlearis immediately in front of the aperture of the cochlear fossula ("psg" in Fig. 6A), although in at least one specimen (CM 10227) the groove is positioned such that the artery crosses the ventromedial face of the cochlear fossula aperture. The proximal stapedial groove begins posterior to the rostral tympanic process and curves anteromedially towards a large oval opening, the oval window or fenestra vestibuli for the footplate of the stapes ("fv" in Fig. 6A), into the posterolateral aspect of the pars cochlearis. The stapedial ratio (of Segall 1970; ratio of length to width of the oval window) for the right fenestra vestibuli of the petrosal in Figure 6 is 1.55; Wysocki (2008) provided length and width measures that produce

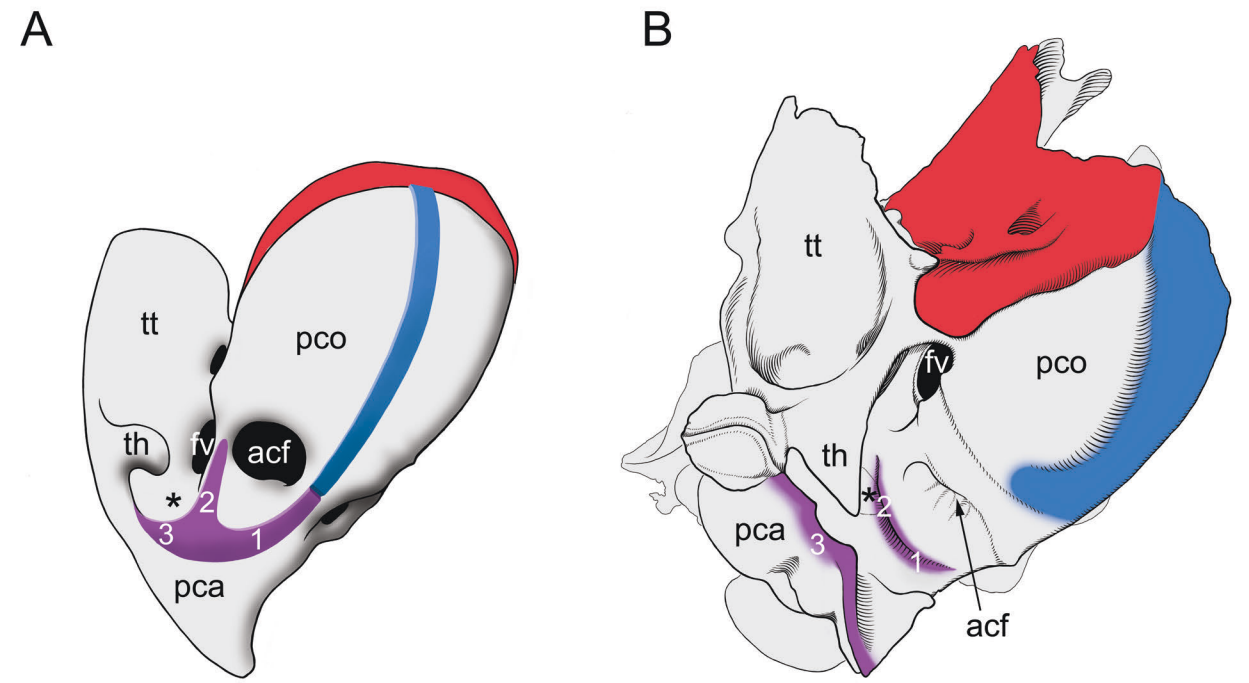

Fig. 5.—Right petrosals in ventral view illustrating outgrowths into the floor and roof of the middle ear. **A,** a hypothetical fetal placental (modified from MacPhee 1981: figs. 2-3); **B,** adult *Rattus norvegicus*, CM teaching collection. The epitympanic wing (red) grows into the middle ear roof and the rostral tympanic process (blue) and caudal tympanic process (purple) grow into the middle ear floor. The caudal tympanic process has three parts: 1, medial; 2, lateral, and medial to the stapedius muscle origin (*); and 3, lateral, and lateral to the stapedius muscle origin (*). Abbreviations: **acf,** aperture of cochlear fossula; **fv,** fenestra vestibuli; **pca,** pars canalicularis; **pco,** pars cochlearis; **th,** tympanohyal; **tt,** tegmen tympani.

a stapedial ratio of 1.76. The fenestra vestibuli is angled such that it is directed posterolateroventrally; its posterior half is recessed within a shallow vestibular fossula. Separating the oval and round windows is a broad bar of bone on the rear of the promontorium, the crista interfenestralis ("ci" in Fig. 6A).

For descriptive purposes, we divide the pars canalicularis into two parts based on their position to the promontorium: one posterolateral and the other anterolateral. In the lateral corner where these two parts meet is a prominent process with a knob-like ventral end, the paroccipital process ("pp" in Fig. 6A; mastoid process of Wahlert 1974). In the intact cranium, the anterolateral surface of the paroccipital process abuts the posttympanic process of the squamosal (Figs. 1–2). The medial surface of the paroccipital process has a groove that represents the posterior terminus of the facial sulcus ("fs" in Fig. 6A) transmitting the facial nerve ("fn" in Fig. 6C).

The posterolateral part of the pars canalicularis has a high rear wall formed by a sharp crest that stretches between the paroccipital process laterally and the paracondylar process of the exoccipital medially ("3" on purple in Fig. 5B; "ctp3" in Fig. 6A). In situ in the cranium in lateral view, the medial end of this crest abutting the paracondylar process projects farther ventrally than the lateral end (Fig. 2). Although the rear surface of the ectotympanic bulla approximates this crest, there is no contact. With an origin at the paroccipital process, this crest represents a part of the caudal tympanic process (primarily the lateral section situated lateral to the stapedius fossa of MacPhee 1981; Fig. 5). Situated deep within the space between the lateral half of this crest and the promontorium is an obliquely-oriented, oval depression wider than long, the stapedius fossa for the origin of the stapedius muscle (Berge and Wirtz 1989b; "sf" in Fig. 6A). This fossa is larger in area than the fenestra vestibuli. Contained within the rim of the stapedius fossa is the lateral semicircular canal ("lsc" in Fig. 4C). Medial to the stapedius fossa and in the plane between that of the fossa and paroccipital process is the cochlear fossula described above (Fig. 6A). The curved, rounded ridge forming the rear wall of the cochlear fossula, parts of the caudal tympanic process mentioned above, attaches to the promontorium on either side of the aperture of the cochlear fossula. The ventral surface of this ridge abuts the ectotympanic bulla ("5" in Fig. 6B) enclosing the cochlear fossula within the middle ear whereas the narrow space posterior to it is extratympanic.

The anterolateral part of the pars canalicularis is dominated by the tegmen tympani ("tt" in Figs. 4A, 5B, 6A), a large, oval, bowl-like structure, longer than wide, with

a footprint roughly comparable to the promontorium. The tegmen tympani tapers anteriorly and projects ventrally, nearly to the same extent as the paroccipital process. The ventral surface of the tegmen tympani can be divided into posteromedial and anterolateral parts. The posteromedial part forms the roof over the malleus and incus ("m" and "i," respectively in Fig. 7B) and the anterolateral part contacts the anterior crus of the ectotympanic bulla ("3" in Fig. 6B; "ac" in Fig. 7A). The space over the mallear-incudal articulation is the epitympanic recess (sensu Klaauw 1931; "er" in Figs. 6A, 7B) and the crus breve or short process of the incus ("cb" in Fig. 7C) sits in a small depression, the fossa incudis ("fi" in Fig. 6A), posterior to and continuous with the epitympanic recess.

The medial and lateral walls of the tegmen tympani are formed by crests that originate posteriorly at the paroccipital process. In the intact cranium, the sharp lateral crest of the tegmen tympani approximates the squamosal (Fig. 1), but is only tightly held to the squamosal just anterior to the posttympanic process ("sqf" in Fig. 6B). The rounded medial crest is the crista parotica ("cp" in Fig. 6A), to which is attached the tympanohyal ("th" in Fig. 6B), the most proximal segment of the hyoid apparatus. In the left petrosal illustrated in Figure 6A, the tympanohyal is broken, exposing the facial sulcus ("fs" in Fig. 6A), which transmits the facial nerve posteriorly to the stylomastoid foramen between the petrosal and ectotympanic (Fig. 2) and then onto a groove on the paroccipital process (Figs. 6A, C). The tympanohyal is reconstructed on the left petrosal in Figures 6B–C, based on the intact one on the right petrosal of the same specimen. The tympanohyal is a triangular prong directed posteromedially and is contacted on its ventral surface by the posterior crus of the ectotympanic ("4" in Fig. 6B; "pc" in Fig. 7A). The crista parotica nearly encloses the facial sulcus in a canal (Fig. 6A), but there is a gap in the medial surface of the crista up to the level of the anterior margin of the fenestra vestibuli (see Fig. 5B). It is through this gap that the distal stapedial artery enters a common canal with the facial nerve (Fig. 6C). Anterior to the level of the fenestra vestibuli, the crista parotica divides into medial and lateral branches (Fig. 6A). The medial branch joins the promontorium, delimiting the fenestra vestibuli from the tensor tympani fossa and the lateral branch joins the low ridge on the epitympanic wing, separating the tensor tympani fossa from the ectotympanic contact ("2" in Fig. 6B). Both the medial and lateral branches contribute to the wall delimiting the rear of the tensor tympani fossa.

Dorsal view.—In a direct dorsal view of the petrosal as it sits in the cranium, the tall crista petrosa divides the bone into dorsolateral and ventromedial surfaces (Fig. 8A). The concave dorsolateral surface lies in the floor of the middle cranial fossa and accommodates the cerebrum ("cs" in Fig. 8A); the ventromedial surface lies in the floor of the caudal cranial fossa and includes the internal acoustic meatus anteriorly (which includes two openings described below, "fas" and "fai" in Fig. 8A) and the subarcuate fossa posteriorly ("saf" in Fig. 8A). The crista petrosa extends the length of the pars canalicularis and pars cochlearis and overhangs the latter anteriorly (Figs. 1, 3); attached to the crista petrosa in life is the tentorium cerebelli (Greene 1935). The anterior portion of the crista petrosa is deflected medially to create a broad trigeminal sulcus on its medial aspect ("trs" in Figs. 3, 6A) for the sensory and motor roots of the trigeminal nerve, cranial nerve V (Greene 1935). On the dorsal aspect of the anterior portion of the crista petrosa is a vascular sulcus that held the superior petrosal sinus, which ran in the fold of the tentorium (Greene 1935; Wysoki 2008; "spss" in Fig. 9A; "sps" in Fig. 9C); this sulcus is not present in all specimens (Fig. 10). The rear of the crista petrosa has a small prong directed anterolaterally ("x" in Fig. 9A) in some specimens, but this is wholly lacking in others (Figs. 8, 10). There is a notch between this prong and the crista petrosa that we interpret as transmitting the superior petrosal sinus (Fig. 9C). The cerebral surface is formed by the crista petrosa medially and the tegmen tympani laterally. At the anterior edge of the cerebral surface is a large, anteriorly directed foramen transmitting the distal stapedial artery from the petrosal ("dsf" in Figs. 8A, 10).

Features in the caudal cranial fossa are better seen in an oblique dorsomedial view (Fig. 9). The internal acoustic meatus ("iam" in Fig. 9B) in the pars cochlearis is shallow with the contained openings and transverse crest ("tc" in Fig. 9A) weakly recessed from the dorsal surface. The thin transverse crest divides the meatus into ventromedial and dorsolateral parts. In the ventromedial part, the foramen acusticum inferius, the major occupant is the cochlear nerve, which coils anteroventrally in the spiral cribriform tract ("sct" in Fig. 9A). At the top of the spiral cribriform tract, medial to the transverse crest is a small, slit-like opening, the foramen singulare ("fsi" in Fig. 9A), transmitting the nerve to the posterior ampulla. Posteromedial to the foramen singulare in the rear of the foramen acusticum inferius is the inferior vestibular area (not visible in the figures), a small cribriform depression transmitting branches of the vestibular nerve. The dorsolateral part of the internal acoustic meatus, the foramen acusticum superius, has a larger anterior opening, the facial canal ("fc" in Fig. 9A), transmitting the facial nerve into the substance of the petrosal, and a smaller, posterior cribriform depression, the superior vestibular area ("sva" in Fig. 9A), for additional branches of the vestibular nerve.

Posterodorsolateral to the internal acoustic meatus in the pars canalicularis is the large, oval (wider than tall) ostium of the subarcuate fossa for the petrosal lobe (paraflocculus) of the cerebellum. The ostium is narrower than the contained fossa, with the width of the ostium comparable to the depth of the fossa. In the cranium, the ostium faces anterodorsomedially (Figs. 3, 8A). Forming much of the rim of the ostium is the gyrus of the anterior semicircular canal (Figs. 8B–C). Posterodorsal to and running parallel to the gyrus of the anterior semicircular canal is a vascular

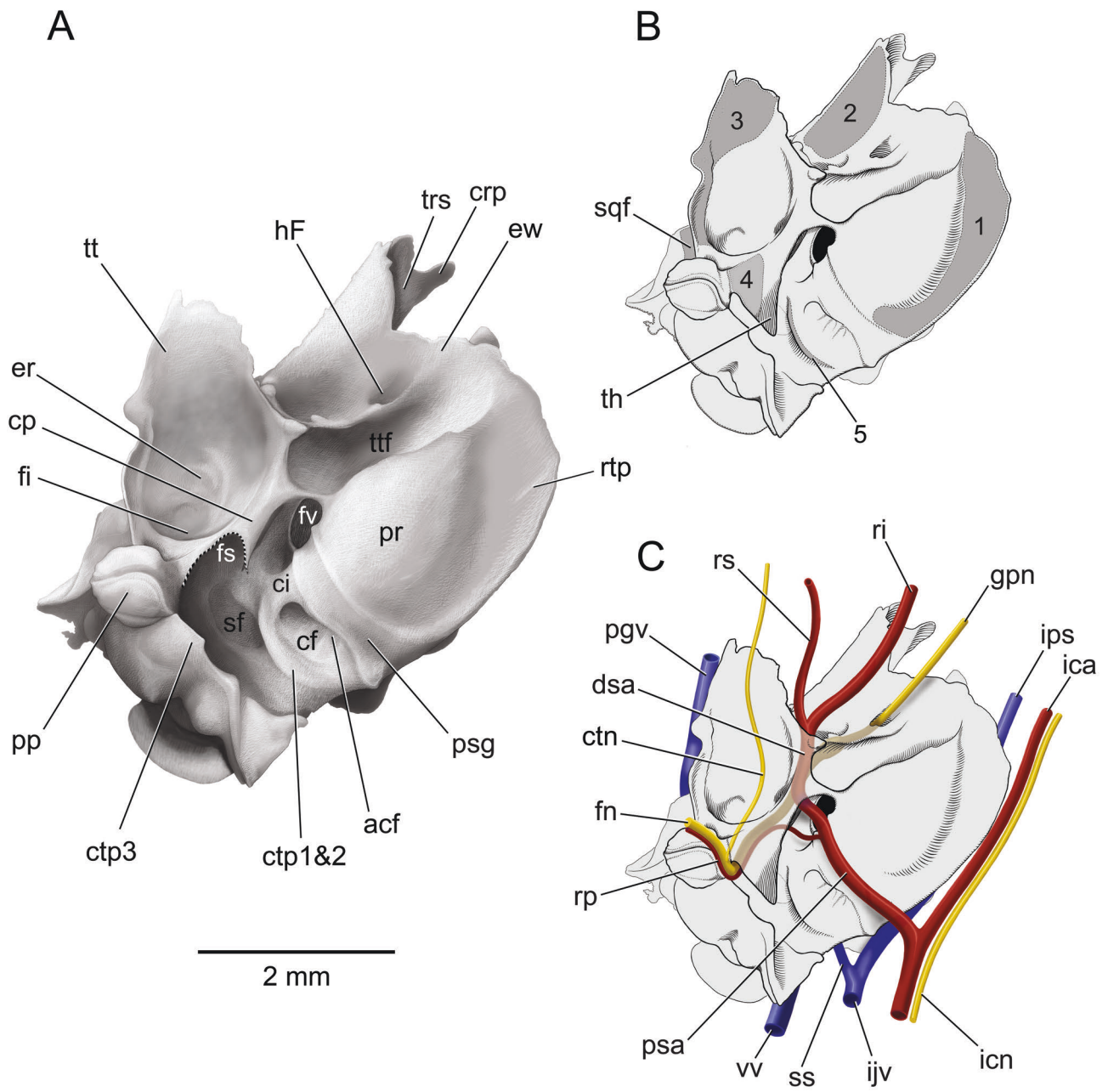

Fig. 6—*Rattus norvegicus*, CM teaching collection, right petrosal in ventral view as positioned in the cranium, anterior to the top of the page. **A,** tone drawing; **B,** line drawing with dark grey indicating contacts with the ectotympanic (numbers 1-5 correspond to surfaces on the ectotympanic in Figure 17) and squamosal; and **C,** line drawing with major neurovascular structures (after Tandler 1899; Greene 1935; Guthrie 1963; Butler 1967; Wible 1984; Szabó 1990, 1995; CM 17504). In A, the tympanohyal was broken with the removal of the ectotympanic bulla, with the break indicated by dotted line; in B and C, the tympanohyal is reconstructed based on the left petrosal of the same specimen. Abbreviations: **acf,** aperture of cochlear fossula; **cf,** cochlear fossula; **ci,** crista interfenestralis; **cp,** crista parotica; **crp,** crista petrosa; **ctn,** chorda tympani nerve; **ctp1&2,** part 1 and 2 of caudal tympanic process (see Fig. 5B); **ctp3,** part 3 of caudal tympanic process (see Fig. 5B); **dsa,** distal stapedial artery; **er,** epitympanic recess; **ew,** epitympanic wing; **fi,** fossa incudis; **fn,** facial nerve; **fs,** facial sulcus; **fv,** fenestra vestibuli; **gpn,** greater petrosal nerve; **hF,** hiatus Fallopii; **ica,** internal carotid artery; **icn,** internal carotid nerve; **ijv,** internal jugular vein; **ips,** inferior petrosal sinus; **pgv,** postglenoid vein; **pp,** paroccipital process; **pr,** promontorium; **psa,** proximal stapedial artery; **psg,** proximal stapedial artery groove; **ri,** ramus inferior; **rp,** ramus posterior; **rs,** ramus superior; **rtp,** rostral tympanic process; **sf,** stapedius fossa; **sqf,** squamosal facet; **ss,** sigmoid sinus; **th,** tympanohyal; **trs,** trigeminal sulcus; **tt,** tegmen tympani; **ttf,** tensor tympani fossa; **vv,** vertebral vein.

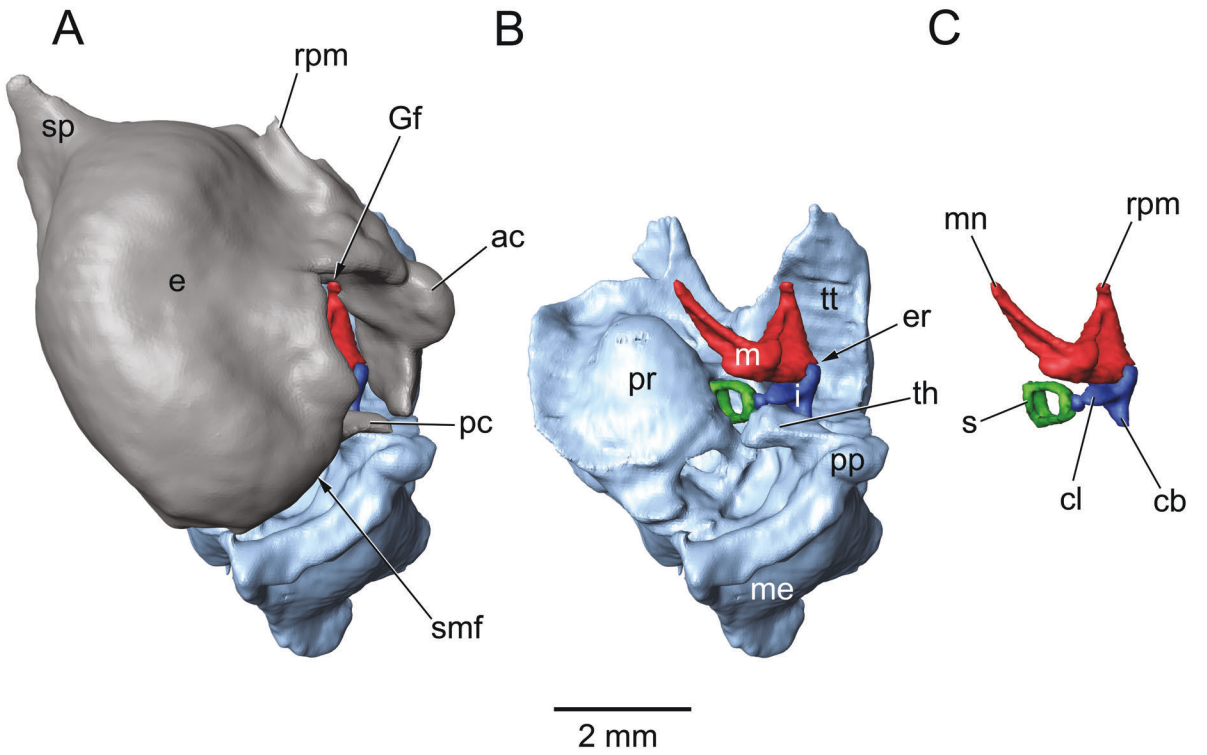

Fig. 7.—*Rattus norvegicus*, TMM M-2272, isosurface rendered from CT data of left ear region in ventral view, tilted medially to visualize the auditory ossicles, anterior to the top of the page. Although shown as separate structures, the rostral process of malleus is fused to the anterior crus of the ectotympanic at the Glaserian fissure, and the tympanohyal is fused to the posterior crus of the ectotympanic. **A,** petrosal (light blue) with ectotympanic (grey), malleus (red), and incus (dark blue) in place; **B,** with ectotympanic removed to expose petrosal and auditory ossicles (stapes in green); and **C,** auditory ossicles alone. Abbreviations: **ac,** anterior crus of ectotympanic; **cb,** crus breve of incus; **cl,** crus longum of incus; **e,** ectotympanic; **er,** epitympanic recess; **Gf,** Glaserian fissure; **i,** incus; **m,** malleus; **me,** mastoid exposure; **mn,** manubrium of malleus; **pc,** posterior crus of ectotympanic; **pp,** paroccipital process; **pr,** promontorium; **rpm,** rostral process of malleus (detached from its fusion to ectotympanic); **s,** stapes; **smf,** stylomstoid foramen; **sp,** styliform process; **th,** tympanohyal; **tt,** tegmen tympani.

sulcus for the sigmoid sinus (Butler 1967; "sss" in Fig. 9A; "ss" in Fig. 9C); CM 29584 has only the faintest indication of the sigmoid sinus sulcus (Fig. 10). Near the medial margin of the subarcuate fossa, the sulcus for the sigmoid sinus sends another sulcus posteriorly ("oevs" in Figs. 9A, 10B) and as it approaches the rear of the petrosal this sulcus is nearly fully enclosed in a canal in that bone; this transmits the occipital emissary vein ("oev" in Fig. 9C) to the mastoid foramen in the suture between the petrosal and supraoccipital (Figs. 2–3). The shelf of pars canalicularis posterior to the sulcus for the sigmoid sinus contacts the supraoccipital in the intact cranium ("sof" in Fig. 9B). The column of bone medial to the subarcuate fossa ostium contains the crus commune, formed where the anterior and posterior semicircular canals join (Fig. 8). The medial aspect of the bony column has a slit-like opening for the endolymphatic duct ("end" in Fig. 8C), the vestibular aqueduct ("va" in Figs. 8A, 9A, 10B). A sharp spine marks the entrance to the aqueduct in some specimens (Figs. 8A, 10B).

Lateral view.—In lateral view of the skull (Fig. 2), the petrosal is exposed in three areas: from anterior to posterior, in the piriform fenestra, in the middle ear, and on the posterolateral braincase. Overlying and laterally obscuring the petrosal between these exposed parts are the ectotympanic, the auditory ossicles, the posttympanic process of the squamosal, and the supraoccipital's contribution to the ventral end of the nuchal crest. Viewing the isolated petrosal (Fig. 11B), it is the tegmen tympani that is visible in the piriform fenestra, the pars cochlearis in the middle ear, and the main pars canalicularis on the posterolateral braincase as the mastoid exposure ("me" in Fig. 11A). Although the ectotympanic is illustrated as fully distinct from the petrosal in Figures 7A and 11A, the posterior crus is fused to the pars canalicularis in the vicinity of the paroccipital process and tympanohyal (Fig. 12), even in juveniles with the M3 erupting (e.g., CM 493). Because of this fusion, removal of the ectotympanic results in breakage on the tympanohyal (Fig. 6A) and/or posterior crus (Fig. 1).

In the oblique anterolateral view in Figure 13, the anterior half of the petrosal is dominated by the large sur-

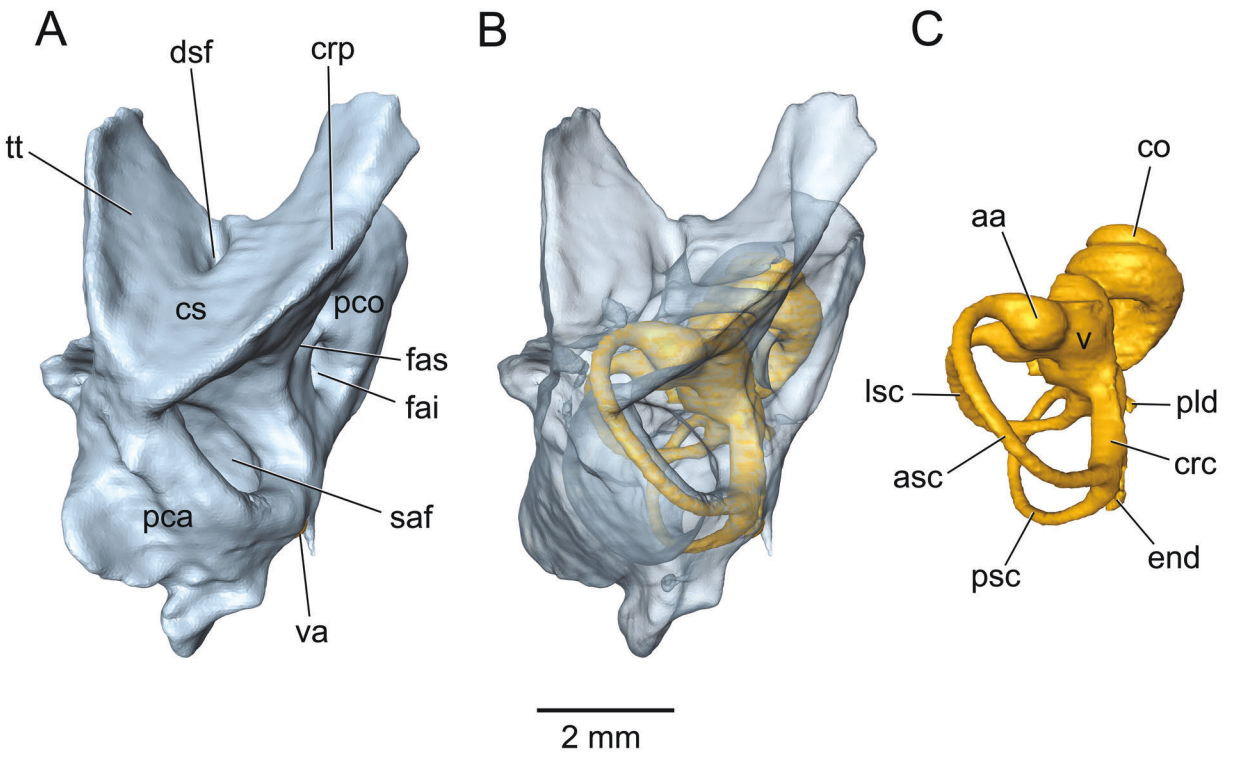

Fig. 8.—*Rattus norvegicus*, TMM M-2272, isosurface rendered from CT data of left petrosal and inner ear in dorsal view as positioned in the cranium, anterior to the top of the page. **A,** petrosal; **B,** transparent petrosal (light blue) showing inner ear (gold); **C,** inner ear. Abbreviations: **aa,** anterior ampulla; **asc,** anterior semicircular canal; **co,** cochlea; **crc,** crus commune; **crp,** crista petrosa; **cs,** cerebral surface; **dsf,** distal stapedial artery foramen; **end,** endolymphatic duct; **fai,** foramen acusticum inferius; **fas,** foramen acusticum superius; **lsc,** lateral semicircular canal; **pca,** pars canalicularis; **pco,** pars cochlearis; **pld,** perilymphatic duct; **psc,** posterior semicircular canal; **saf,** subarcuate fossa; **tt,** tegmen tympani; **v,** vestibule; **va,** vestibular aqueduct.

face contacting the cerebrum. In this figured specimen, the cerebral surface is rough with many small longitudinal ridges, but in others (e.g., CM 29584, TTM M-2272) this surface is smooth (Figs. 8A, 10). The superior petrosal sinus runs in the variably present longitudinal sulcus at the top of the cerebral surface (Greene 1935; Wysoki 2008; Figs. 13A, C), and the sharp crista petrosa above that sulcus delimits the medial boundary of the cerebral surface. The crista petrosa increases in height posteriorly to its high point on the pars canalicularis. From there, a much lower crest descends sharply anterolaterally onto the dorsal aspect of the tegmen tympani and delimits the lateral boundary of the cerebral surface. At the apex of this crest is the variably present prong ("x" in Fig. 13A) described above. On the lateral surface of this crest is a sulcus for the postglenoid vein ("pgvs" in Fig. 13A; "pgv" in Fig. 13C), which can be followed posterodorsally where it intersects with the sulcus for the sigmoid sinus. Some specimens (e.g., CM 29584, TTM M-2272) have a well-developed foramen within the postglenoid vein sulcus ("vf" in Figs. 11A, 12B), which is lacking in others (Fig. 13A). Based on the CT scans of TTM M-2272, the foramen ends in the substance of the pars canalicularis and likely transmitted a vein given its relationship to the postglenoid vein. Posterior to the postglenoid vein sulcus is the quadrangular-shaped facet for the squamosal bone ("sqf" in Fig. 13B). Between the cerebral surface and the promontorium, the foramen transmitting the distal stapedial artery from the petrosal is barely visible in the figured specimen ("dsf" in Fig. 13A). However, in others (e.g., CM 29584, TTM M-2272), this foramen opens within the cerebral surface (Figs. 8A, 10).

Medial view.—The petrosal in situ in the skull is shown in medial view in Figure 3, whereas the isolated bone is illustrated in an oblique dorsomedial view in Figure 14B. With the ectotympanic in place (Fig. 14A), two conduits into the posterior aspect of the middle ear are discernible. The more posterior conduit (not labeled in Fig. 14A) is between the part of the caudal tympanic process abutting the paracondylar process of the exoccipital ("ctp3" in Fig. 14A) and the ectotympanic. We have not found named structures passing through this conduit in the rodent literature; however, in other mammals, this represents the passageway for the auricular branch of the vagus nerve and, therefore, represents the mastoid canaliculus (MacPhee

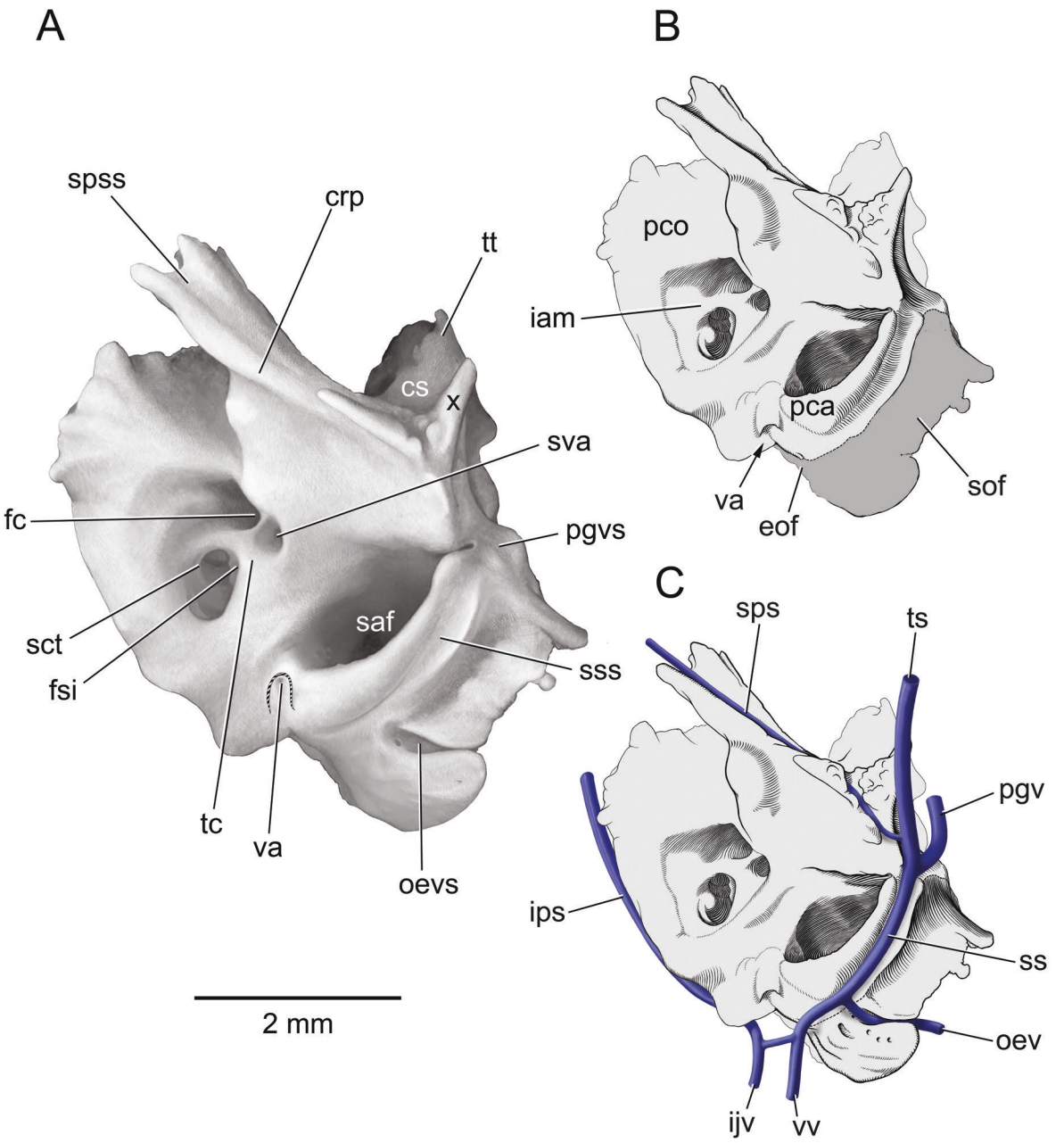

Fig. 9.—*Rattus norvegicus*, CM teaching collection, right petrosal in oblique dorsomedial view, anterior to the top of the page. **A,** tone drawing; **B,** line drawing with dark grey indicating contacts with supraoccipital dorsally and exoccipital medially; **C,** line drawing with major veins (after Greene 1935; Butler 1967; Szabó 1990, 1995). In A, the bone around the vestibular aqueduct was broken, with the break indicated by dotted line; in B and C, the bone hiding the vestibular aqueduct aperture is reconstructed based on the left petrosal of the same specimen. Abbreviations: **crp,** crista petrosa; **cs,** cerebral surface; **eof,** exoccipital facet; **fc,** facial canal; **fsi,** foramen singular; **iam,** internal acoustic meatus; **ijv,** internal jugular vein; **ips,** inferior petrosal sinus; **oev,** occipital emissary vein; **oevs,** occipital emissary vein sulcus; **pca,** pars canalicularis; **pco,** pars cochlearis; **pgv,** postglenoid vein; **pgvs,** postglenoid vein sulcus; **saf,** subarcuate fossa; **sct,** spiral cribriform tract; **sof,** supraoccipital facet; **sps,** superior petrosal sinus; **spss,** superior petrosal sinus sulcus; **ss,** sigmoid sinus; **sss,** sigmoid sinus sulcus; **sva,** superior vestibular area; **tc,** transverse crest; **ts,** transverse sinus; **tt,** tegmen tympani; **va,** vestibular aqueduct; **vv,** vertebral vein; **x,** anterolaterally directed prong from crista petrosa.

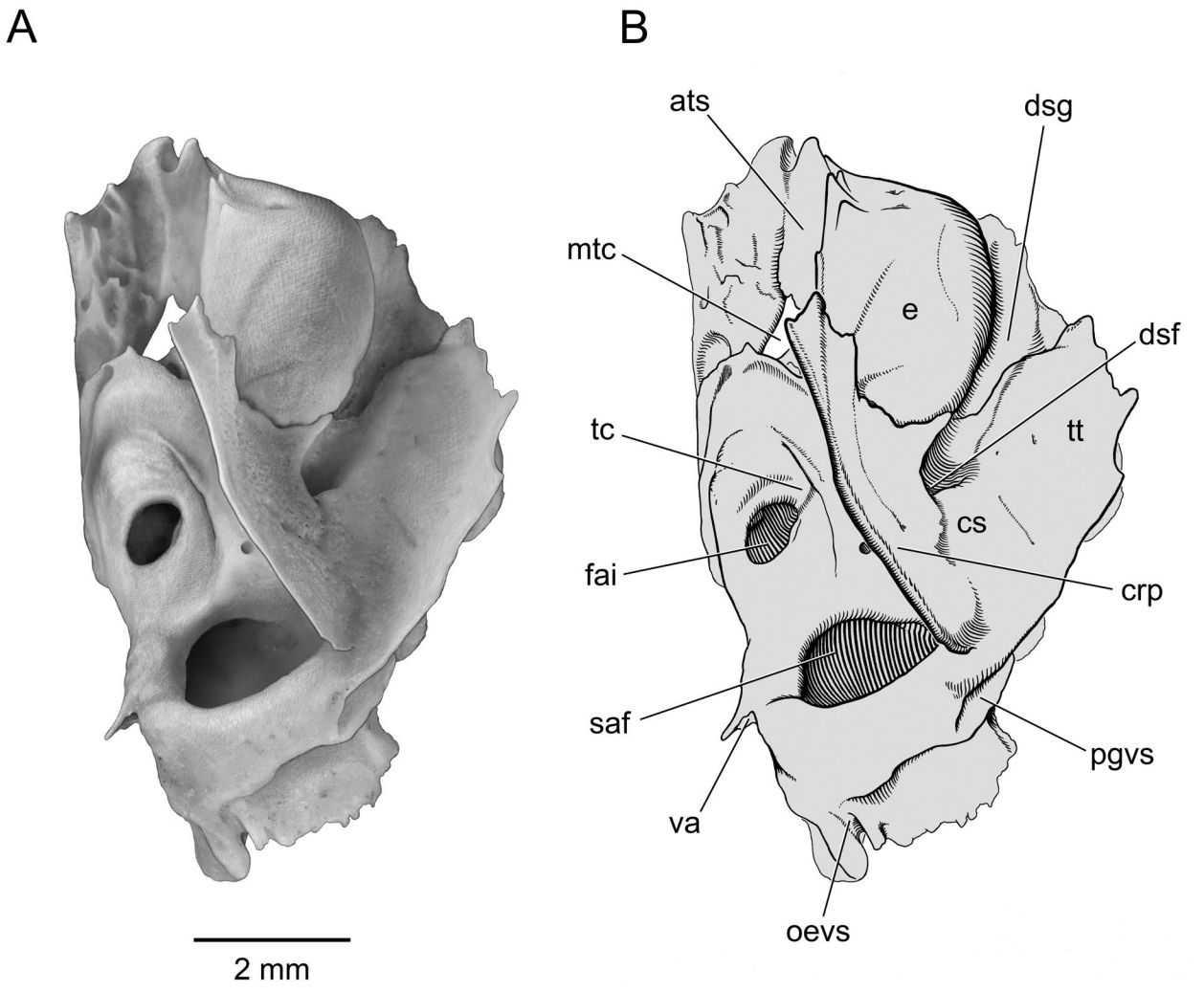

Fig. 10.—*Rattus norvegicus,* CM 29584, right petrosal and ectotympanic in oblique dorsolateral view, anterior to the top of the page. **A,** drawing on photo; **B,** line drawing. Abbreviations: **ats,** auditory tube sulcus; **crp,** crista petrosa; **cs,** cerebral surface; **dsf,** distal stapedial artery foramen; **dsg,** distal stapedial artery groove; **e,** ectotympanic; **fai,** foramen acusticum inferius; **mtc,** musculotubal canal; **oevs,** occipital emissary vein sulcus; **pgvs,** postglenoid vein sulcus; **saf,** subarcuate fossa; **tc,** transverse crest; **tt,** tegmen tympani; **va,** vestibular aqueduct.

1981; Wible and Spaulding 2013). The anterior conduit into the middle ear is the foramen between the pars cochlearis and ectotympanic transmitting the proximal stapedial artery onto the promontorium ("psf" in Fig. 14A). Dorsal to the foramen for the proximal stapedial artery is a smaller opening into the pars cochlearis, the cochlear canaliculus for the perilympatic duct ("coc" in Fig. 14A). Although the cochlear canaliculus is recessed dorsally from the ventral surface of the pars cochlearis, it is visible through the jugular foramen in the skull (e.g., CM 10227).

There is a large opening in the medial aspect of the pars canalicularis that we have not found reference to in the rodent literature. It opens through the medial wall of the subarcuate fossa and we call here the subarcuate fenestra ("sfe" in Fig. 14A). As is apparent from the transparent petrosal in Figure 14B, the subarcuate fenestra passes through the middle of the arc of the posterior semicircular canal. With the petrosal in situ in the skull, the subarcuate fenestra faces the exoccipital but is not firmly pressed against that bone. All specimens in which we were able to visualize this area have a fenestra (e.g., CM 10227, 29584) but it is variable in size and shape. McClure and Daron (1971) studied the development of the subarcuate fossa in the King-Holtzman strain of laboratory rats. In the adults they found no similar perforation, but in this position in embryos (i.e., within the arc of the posterior semicircular canal), they reported a cord of loose, vascularized connective tissue, with the vascular elements draining into the

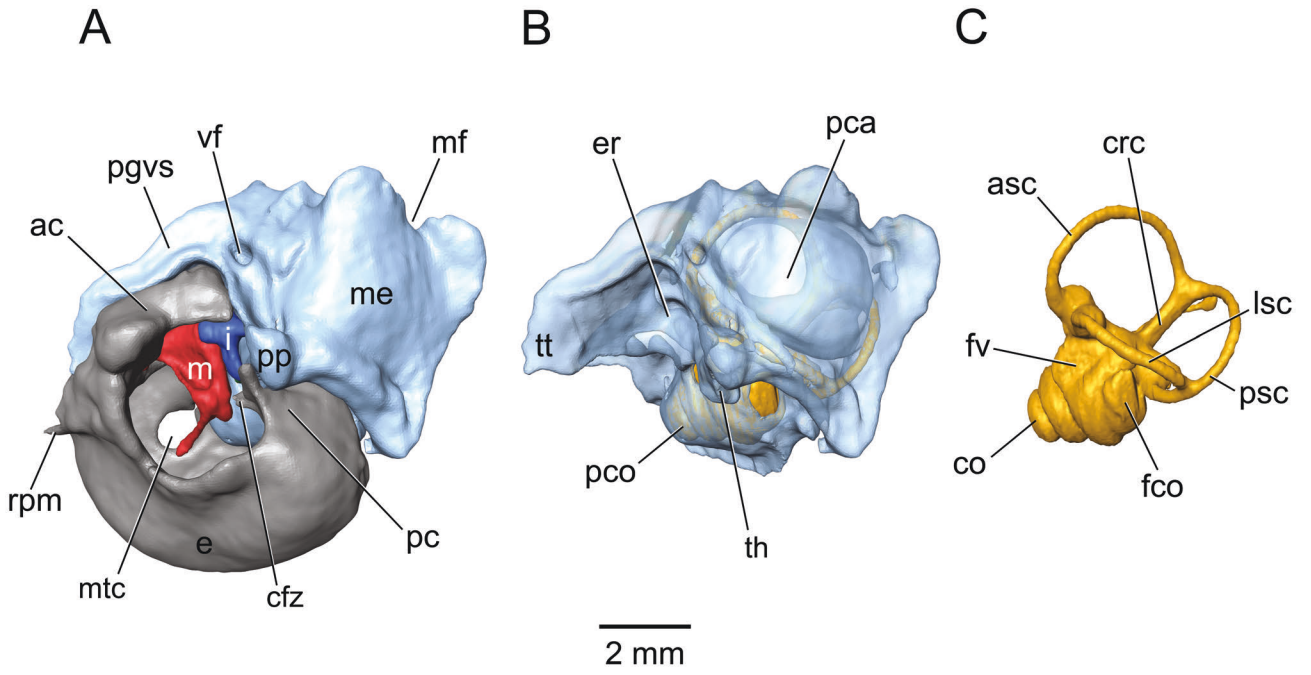

Fig. 11.—*Rattus norvegicus*, TMM M-2272, isosurface rendered from CT data of left ear region in lateral view as positioned in the cranium, anterior to the left. As noted with Figure 7, the rostral process of the malleus is fused to the anterior crus of the ectotympanic and the tympanohyal is fused to the posterior crus of the ectotympanic. **A,** petrosal (light blue), ectotympanic (grey), malleus (red), and incus (dark blue); **B,** transparent petrosal (light blue) showing inner ear (gold); **C,** inner ear. Abbreviations: **ac,** anterior crus of ectotympanic; **asc,** anterior semicircular canal; **cfz,** chordaforsatz; **co,** cochlea; **crc,** crus commune; **e,** ectotympanic; **er,** epitympanic recess; **fco,** fenestra cochleae; **fv,** fenestra vestibuli; **pgvs,** postglenoid vein sulcus; **i,** incus; **lsc,** lateral semicircular canal; **m,** malleus; **me,** mastoid exposure; mf, mastoid foramen; **mtc,** musculotubal canal; **pc,** posterior crus of ectotympanic; **pca,** pars canalicularis; **pco,** pars cochlearis; **pp,** paroccipital process of petrosal; **psc,** posterior semicircular canal; **rpm,** rostral process of malleus (fused to ectotympanic); **th,** tympanohyal; **tt,** tegmen tympani; **vf,** venous foramen.

sigmoid sinus. Although this vascular connection disappeared in later ontogenetic stages and its "aperture" ultimately ossified, it did so later than the surrounding bone. Based on the observations of McClure and Daron (1971), we suggest that the subarcuate fenestra in our sample results from a failure to fully ossify this area and that it is closed by a connective tissue membrane and does not transmit structures.

Also visible in this oblique dorsomedial view is a longitudinal vascular sulcus on the medial aspect of the pars cochlearis ("ipss" in Fig. 14A). This transmits the inferior petrosal sinus (Greene 1935; "ips" in Fig. 6C) from the cavernous sinus around the hypophysis to the internal jugular vein. This sulcus is not visible in direct medial view in the skull because it faces the basioccipital (Fig. 3).

Ectotympanic, Malleus, Incus, and Stapes

The paired ectotympanics (tympanics of Greene 1935) provide attachment for the tympanic membranes and form the floors of the middle ears and partial floors for the external ears. The paired mallei articulate with the incudes, attach to the tympanic membranes, and are fused to the ectotympanics through their rostral processes. The paired incudes articulate with the stapes, which in turn occupy the fenestrae vestibuli of the pars cochlearis. Because of the intimate relationship between these bones, we consider them together here. Mason (2001: appendix and references therein) recorded measurements of these bones in *R. norvegicus*, including mass of the stapes (0.090 mg) and combined mass of the malleus + incus (1.468 mg), the malleus and incus lever arms (2.13 mm and 0.88 mm, respectively) and their ratio (2.42), and the area of the stapedial footplate (0.356 mm^2) and pars tensa of the tympanum (7.83 mm^2). Lavender et al. (2011: table 1) recorded the moment of inertia of the malleus (0.170 mg mm^2) and incus (1.377 mg mm^2).

In early ontogenetic stages, the rat malleus has a well-developed rostral process situated adjacent to the anterior crus of the ectotympanic and forming from a separate intramembranous ossification, the goniale (Youssef 1966), that fuses to the malleus in later stages ("rpm" in 14-day-old mouse in Fig. 15A; Anthwal et al. 2013). However, the adult rat malleus (in red in Fig. 15B) is usually shown with a reduced rostral process (e.g., Albuquerque et al. 2009: fig. 4B; Salih et al. 2012: fig. 1d; Maynard and Downes 2019: fig. 23.3), which is reported to articulate with the

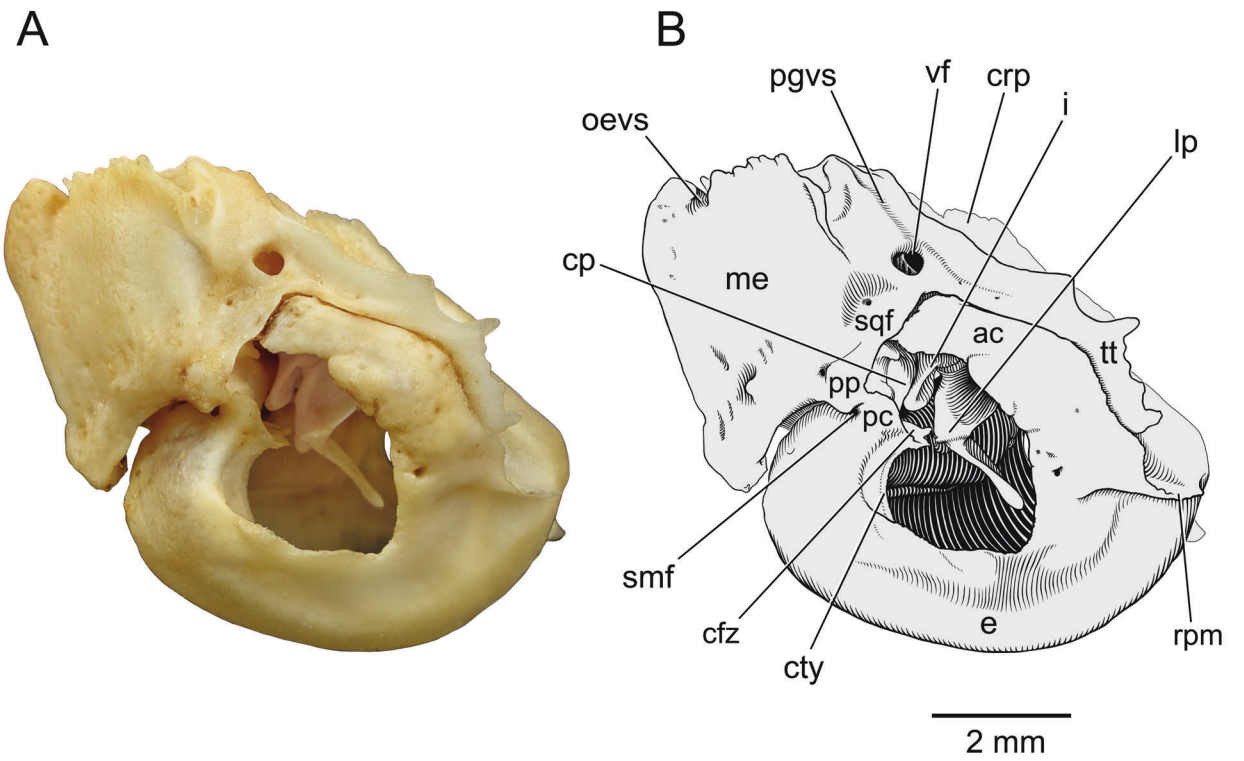

Fig. 12.—*Rattus norvegicus*, CM 29584, right petrosal, ectotympanic, and auditory ossicles in lateral view as positioned in the cranium, anterior to the right. **A,** photograph; **B,** line drawing. Abbreviations: **ac,** anterior crus of ectotympanic; **cfz,** chordaforsatz; **cp,** crista parotica; **crp,** crista petrosa; **cty,** crista tympanica; **e,** ectotympanic; **i,** incus; **lp,** lateral process of malleus; **me,** mastoid exposure; **oevs,** occipital emissary vein sulcus; **pc,** posterior crus of ectotympanic; **pgvs,** postglenoid vein sulcus; **pp,** paroccipital process of petrosal; **rpm,** rostral process of malleus (fused to ectotympanic); **smf,** stylomastoid foramen; **sqf,** squamosal facet; **tt,** tegmen tympani; **vf,** venous foramen.

ectotympanic (Hellström et al. 1982:350). In contrast, Fleischer (1973: fig. 31) illustrated an elongate rostral process in *Rattus rattus* (Linnaeus, 1758) and reported it as "fused firmly with the tympanic" (Fleischer 1978: 51), characteristic of his microtype ossicle category (versus freely mobile; see also Lavender et al. 2011; Mason 2015).

In our study, we encountered juvenile brown rat specimens that confirm Fleischer's claim, i.e., having an elongate rostral process that is set off from the ectotympanic by sutures (e.g., CM 493, 21415). In contrast, in adults the rostral process and ectotympanic are seamlessly fused. To illustrate the relationship between the rostral process and the ectotympanic, a dorsal view is best, which requires that the petrosal and ectotympanic be isolated from the skull. The CM holdings of brown rat juveniles contained no such examples, but we found several suitable juveniles of the black rat, *Rattus rattus*, one of which is illustrated in Figure 16 (CM 101347). Its rostral process is a spoon-shaped bony lamina (Fig. 15B) dorsal to the anterior crus of the ectotympanic (Fig. 16). The bowl of the spoon is flat with a slightly raised lateral lip and is partially fused to the ectotympanic along its posteromedial border. Overlying and obscuring the proximal part of the bowl and the handle of the spoon is the tegmen tympani. Continuity between the part of the malleus in the middle ear and the extratympanic part dorsal to the tegmen tympani is via the Glaserian fissure ("Gf" in Fig. 7A), which transmits the chorda tympani nerve from the middle ear in mammals (Klaauw 1931). Between the anterior tip of the tegmen tympani and the rostral process is a narrow gap that represents the rostral continuation of the Glaserian fissure (Fig. 16).

For the adult brown rat, an isolated right ectotympanic is illustrated in two views in Figure 17, a left ectotympanic in contact with the petrosal is shown in Figures 7A, 11A, and 14A, and a right ectotympanic in situ in the skull is shown in Figures 1–3. In all of these adults, the ectotympanic is fused to the rostral process of the malleus, that is, the bowl and the adjacent part of the handle of the spoon. In CM 10227 and TTM M-2272, the rostral process is continuous with the rest of the malleus (the different colors applied to the ectotympanic and malleus in Figs. 7A and 11A masks this continuity), whereas in the CM teaching collection brown rat (Fig. 17), the rostral process has been isolated from the rest of the malleus through breakage. In its embryonic form, the rat ectotympanic is a simple U-shaped rod with a very broad gap between the crurae, the tympanic incisure, directed posterolaterally (Youssef 1966). This dramatically changes by the adult with the ec-

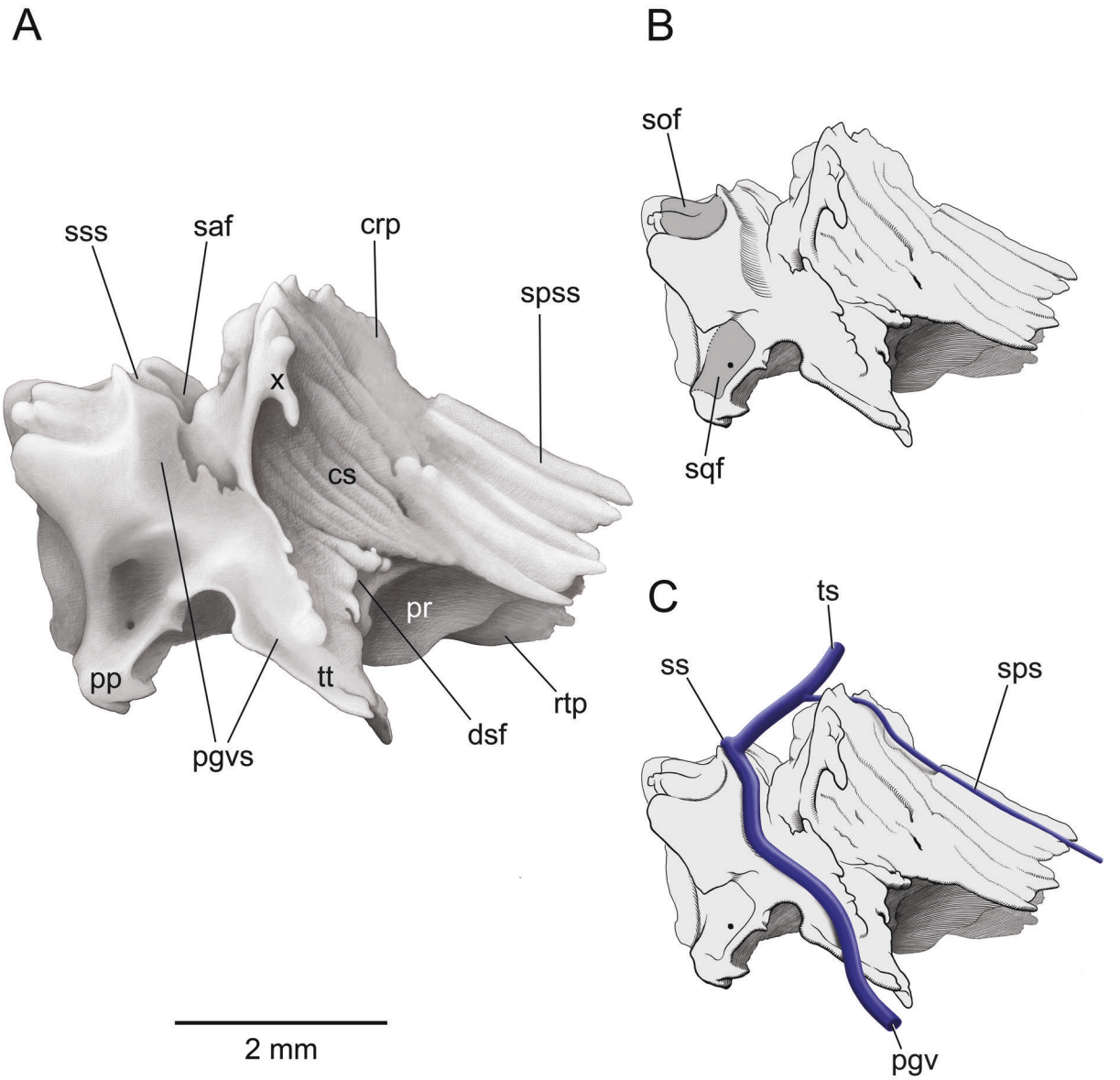

Fig. 13.—*Rattus norvegicus*, CM teaching collection, right petrosal in oblique lateral view, anterior to the right. **A,** tone drawing; **B,** line drawing with dark grey indicating contacts with supraoccipital and squamosal; **C,** line drawing with major veins (after Butler 1967; Szabó 1990, 1995). Abbreviations: **crp,** crista petrosa; **cs,** cerebral surface; **dsf,** distal stapedial artery foramen; **pco,** pars cochlearis; **pgv,** postglenoid vein; **pgvs,** postglenoid vein sulcus; **pp,** paroccipital process; **pr,** promontorium; **rtp,** rostral tympanic process; **saf,** subarcuate fossa; **sof,** supraoccipital facet; **sps,** superior petrosal sinus; **spss,** superior petrosal sinus sulcus; **sqf,** squamosal facet; **ss,** sigmoid sinus; **sss,** sigmoid sinus sulcus; **ts,** transverse sinus; **tt,** tegmen tympani; **x,** anterolaterally directed prong from crista petrosa.

totympanic shaped like a bowl with conduits for structures gaining access to the middle ear, with prominences and facets contacting the tympanic surface of the petrosal, and with a reduced tympanic incisure ("ti" in Fig. 17A).

In dorsal view (Fig. 17A), the ectotympanic's five separate areas of contact with the petrosal are all visible. The largest ("1" in Fig. 17A) on the medial side is slightly convex and contacts the concave surface of the rostral tympanic process (Fig. 6B). A distinct lip is present on its extratympanic margins. It is flanked posteriorly by a deep groove for the proximal stapedial artery, marking that vessel's entrance into the middle ear between the ectotympanic and petrosal near the jugular foramen (Figs. 1, 14A), and anteriorly by the large musculotubal canal for the auditory tube ("mtc" in Figs. 14A, 16–17), which is roofed dorsally by the styliform process. The auditory tube opening is oval

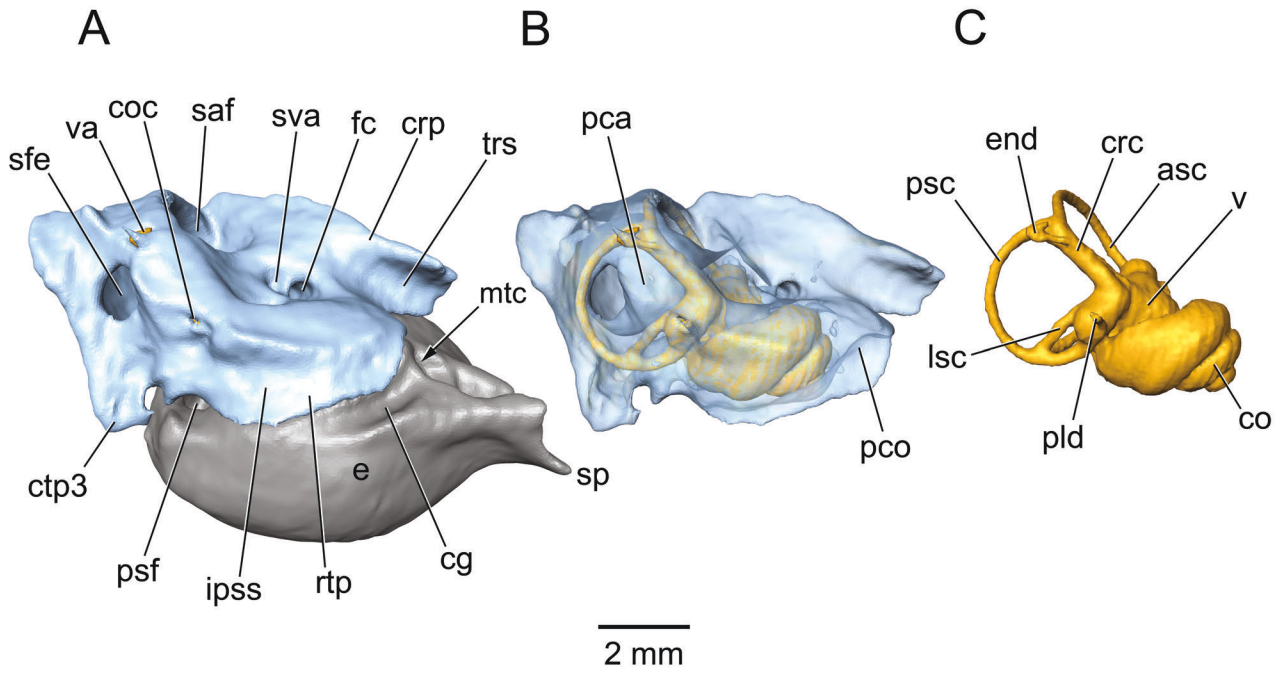

Fig. 14.—*Rattus norvegicus*, TMM M-2272, isosurface rendered from CT data of left ear region in oblique medial view, anterior to the right. **A,** petrosal (light blue) and ectotympanic (gray); **B,** transparent petrosal (light blue) showing inner ear (gold); **C,** inner ear. Abbreviations: **asc,** anterior semicircular canal; **cg,** carotid groove; **co,** cochlea; **coc,** cochlear canaliculus; **crc,** crus commune; **crp,** crista petrosa; **ctp3,** part 3 of caudal tympanic process (see Fig. 5B); **e,** ectotympanic; **end,** endolymphatic duct; **fc,** facial canal; **ipss,** inferior petrosal sinus sulcus; **lsc,** lateral semicircular canal; **mtc,** musculotubal canal; **pca,** pars canalicularis; **pco,** pars cochlearis; **pld,** perilymphatic duct; **psc,** posterior semicircular canal; **psf,** proximal stapedial artery foramen; **rtp,** rostral tympanic process of petrosal; **saf,** subarcuate fossa; **sfe,** subarcuate fenestra; **sp,** styliform process; **sva,** superior vestibular area; **trs,** trigeminal sulcus; **v,** vestibule; **va,** vestibular aqueduct.

(wider than high) and primarily formed by the ectotympanic, with only a small contribution dorsally from the pars cochlearis. Lateral to the auditory tube opening, on the anterior crus, is the next largest contact area ("2" in Fig. 17A), which is strongly convex and fits into the concave depression on the epitympanic wing of the petrosal (Fig. 6B). It is flanked anteromedially by the sulcus for the greater petrosal nerve ("gpns" in Fig. 17A), which runs forward from the hiatus Fallopii (Fig. 6A), and posteriorly by the narrow Glaserian fissure for the chorda tympani nerve ("Gf" in Fig. 17A). Posterior to the Glaserian fissure, on the distalmost anterior crus is an irregular convex surface ("3" in Fig. 17A), which contacts the anterolateral aspect of the tegmen tympani's ventral surface and forms the lateral wall of the epitympanic recess and fossa incudis (Fig. 6B). The posterolateral aspect of this irregular surface has a minor contact with the medial aspect of the posttympanic process of the squamosal (Fig. 2). The remaining two smaller contact surfaces are on the posterior crus. The medial one is a narrow, curved convex surface ("5" in Fig. 17A) abutting the part of the caudal tympanic process posterior to the cochlear fossula (Fig. 6B). Lateral to it, at the distalmost posterior crus ("4" in Fig. 17A) is the irregular surface that fuses to the tympanohyal (Fig. 6B) and, therefore, is usually broken in isolated ecotympanics. Between these two contact surfaces is a broad sulcus transmitting the facial nerve from the middle ear ("fs" in Fig. 17A), which marks the position of the stylomastoid foramen in the skull (Figs. 2, 7A). In the medial wall of the facial sulcus (hidden by contact area 5 in Fig. 17A) is a small foramen that transmits the chorda tympani nerve from its origin on the facial nerve into the middle ear ("fct" in Fig. 17A).

Part of the intrabullar surface of the ectotympanic is visible in dorsal view. Extending from contact area 3 on the anterior crus to near the end of the posterior crus is the prominent crista tympanica ("cty" in Fig. 17A), which forms the internal wall of the sulcus tympanicus ("sty" in Fig. 17A), the site of attachment for the tympanum. External to the sulcus tympanicus is the floor of the recessus meatus ("rem" in Fig. 17A; recessus meatus acustici externi of Klaauw 1931), the part of the bulla that floors part of the membranous external acoustic meatus. The incorporation of the recessus meatus into the bulla results from the oblique orientation of the tympanum, which as measured in the CT scans is 70° from the horizontal.

In ventral view (Fig. 1), the part of the bulla flooring the middle ear is reniform with thinner, translucent bone. Marking its lateral boundary is a thicker, curved line indicating the crista tympanica ("cty" in Fig. 1). Lateral to the position of the crista tympanica is the part of the bulla

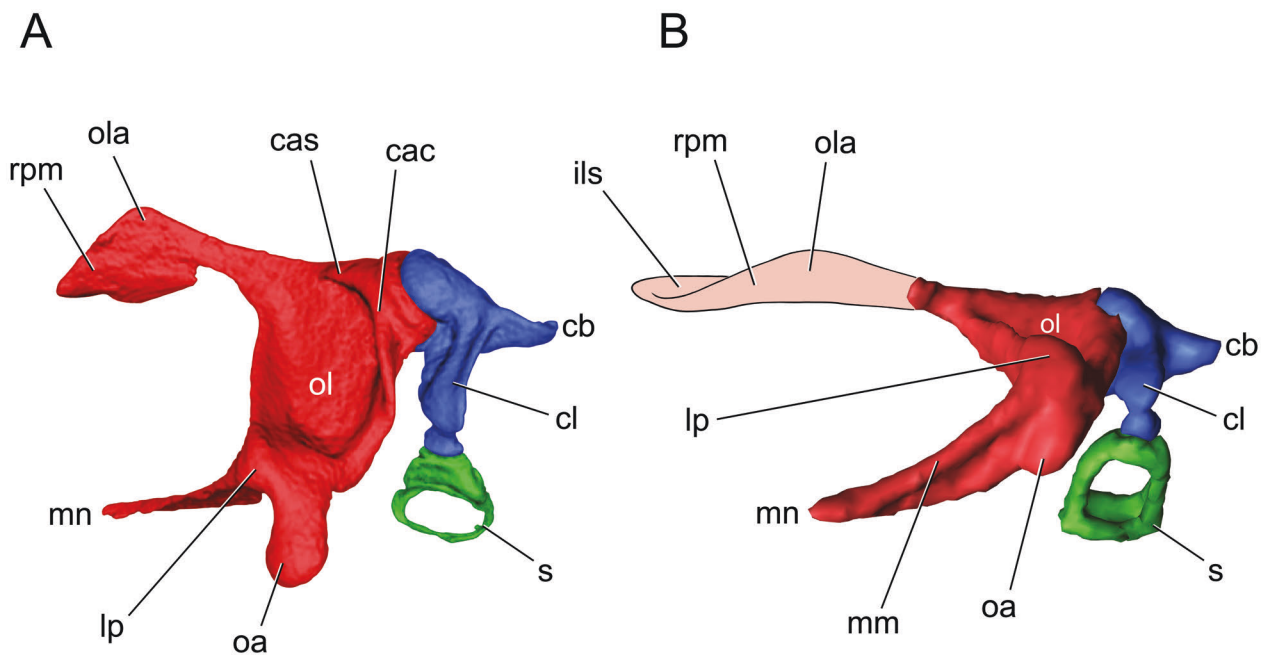

Fig. 15.—Left auditory ossicles, isosurfaces rendered from CT data in oblique ventrolateral view, anterior to the left. **A,** 14 day-postnatal mouse (modified from Anthwal et al. 2013: fig. 1D; no scale provided); **B,** *Rattus norvegicus*, TMM M-2272 (for scale, see Fig. 18). In B, the dark red part of the malleus is as the bone is figured in, for example, Albuquerque et al. (2009: fig. 4B) and Salih et al. (2012: fig. 1d); the elongate rostral process is reconstructed in light red based on that structure in juveniles (e.g., CM 101347), with the proportions fit to the adult. Abbreviations: **cac,** capitular crest; **cas,** capitular spine; **cb,** crus breve; **cl,** crus longum; **ils,** interlamellar sulcus; **lp,** lateral process of malleus; **mm,** membrane margin of manubrium; **mn,** manubrium; **oa,** orbicularis apophysis; **ol,** osseous lamina; **ola,** outer lamella; **rpm,** rostral process of malleus; **s,** stapes.

flooring the recessus meatus. Its lateral margin has some slight lipping that represents the floor to the proximal part of the cylindrical external meatus. The ectotympanic is much broader across the anterior crus than the posterior crus (Fig. 7A). Both crurae are narrow at their distal ends, but the anterior crus has a prominent boss extending lateral to the plane of the tegmen tympani ("ac" label is on this boss in Fig. 7A). The narrow tympanic incisure is roofed entirely by the pars canalicularis anterior to the paroccipital process. Two variable processes are found along the anterior margin of the bulla. At the anteromedial corner is the styliform process of the ectotympanic ("sp" in Fig. 17; muscular process of Popesko et al. 1992), which floors the auditory tube. This variably is sharply pointed (Fig. 7A), more rounded (Fig. 17), or irregular (Fig. 1). At the anterolateral corner is the terminus of the rostral process of the malleus, which as noted above is fused to the ectotympanic in the adult. This may be gently rounded and not protruding far from the adjacent ectotympanic ("rpm" in Figs. 12B, 17B), a short sharp spine ("rpm" in Figs. 7A, 11A), or an elongate sharp spine extending into the piriform fenestra ("rpm" in Fig. 1). Medial to the distal end of the rostral process is the groove in the ectotympanic transmitting the distal stapedial artery after it leaves the middle ear ("dsg" in Figs. 16, 17B).

A last outgrowth on the bulla to consider is the chordaforsatz, a structure reported in various mammals related to the course of the chorda tympani nerve in the middle ear (Bondy 1907; Klaauw 1923, 1931). In the brown rat, the chordafortsatz ('fortsatz' is German for 'process') is a short, thin shelf reaching anteriorly from the distal end of the posterior crus ("cfz" in Figs. 11A, 12B, 17B) towards the malleus, near its lateral process ("lp" in Fig. 12B). The sharp crest on the ventrolateral aspect of this shelf is the terminus of the crista tympanica (Fig. 12) and running on the dorsal aspect of the shelf is the chorda tympani nerve from its posterior foramen of entrance described above. The term chordaforsatz has been applied to non-homologous structures arising from the petrosal, the ectotympanic, the squamosal, and the element of Spence, an independent cartilage that may fuse to a neighboring bone. We are uncertain of the embryonic origin of the chordafortsatz in the brown rat, but given its relationship to the crista tympanica, we interpret it as an outgrowth of the posterior crus. The term caudal chordafortsatz has been used (e.g., Mason 2013, 2015; Maynard and Downes 2019) for the structure in rodents, including the rat, that we describe here as the chordaforsatz. Adding 'caudal' as a descriptor is unnecessary as, to our knowledge, there is no rostral chordafortsatz.

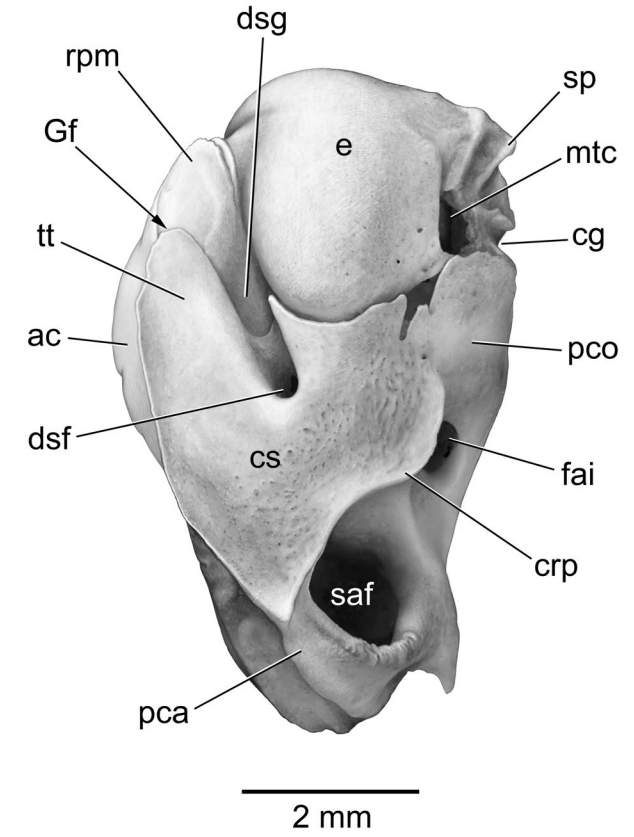

Fig. 16.—*Rattus rattus*, CM 101347, left petrosal, ectotympanic, and malleus in oblique dorsomedial view, drawing on photograph, anterior to the top of the page. The rostral process of the malleus is separated from the underlying ectotympanic by sutures laterally and anteromedially, but is fused to the ectotympanic posteromedially. Abbreviations: **ac,** anterior crus of ectotympanic; at, **cg,** carotid groove; **crp,** crista petrosa; **cs,** cerebral surface; **dsf,** distal stapedial artery foramen; **dsg,** distal stapedial artery groove; **e,** ectotympanic; **fai,** foramen acusticum inferius; **Gf,** Glaserian fissure; **mtc,** musculotubal canal; **pca,** pars canalicularis; **pco,** pars cochlearis; **rpm,** rostral process of malleus; **saf,** subarcuate fossa; **sp,** styliform process; **tt,** tegmen tympani.

Although the malleus (minus the distal rostral process), incus, and stapes have been treated previously by other authors (e.g., Albuquerque et al. 2009; Salih et al. 2012), we include descriptions of them here for the sake of completeness. The malleus of TTM M-2272 with reconstructed distal rostral process is illustrated in oblique ventrolateral view in Figure 15B, and without the reconstructed distal rostral process in lateral and medial views in Figures 18A and B, respectively. The head of the malleus ("hm" in Figs. 18A–B) is dorsoventrally compressed and is piriform shaped in dorsal view with the broader part articulating with the incus. The head is not delimited by a capitular crest or capitular spine as occurs in the mouse ("cac" and "cas," respectively, in Fig. 15A). The head has two convex articular surfaces for the incus separated by a tiny groove and set off from each other at a 100° angle, with the superior surface slightly larger than the inferior ("suaf" and "iaf" in Fig. 18A). Adjacent to the latter articular surface is the thick, fairly straight neck of the malleus ("nm" in Figs. 18A–B) that ends at the manubrial base. The manubrium ("mn" in Figs. 15B, 18A–B) is saber-shaped, anteroposteriorly compressed, with a very slightly spatulated tip. The membrane margin of the manubrium on the lateral aspect is prominent ("mm" in Fig. 15B) compared to that in the mouse (Fig. 15A). In addition to the manubrium, the manubrial base supports three prominences. The largest, the lateral process ("lp" in Figs. 12B, 15B, 18A), on the lateral surface projects into the tympanum; the smallest on the medial surface is the muscular process for the attachment of the tensor tympani muscle ("mptt" in Fig. 18B); and the last is the orbicularis apopohysis ("oa" in Figs. 15B, 18A–B), projecting ventrally, which is much smaller than that in the mouse (Fig. 15A). The orbicular apophysis has been shown to be derived from the second branchial arch in mice in contrast to the first arch origin of the remainder of the malleus (O'Gorman 2005; see Mason 2013). Between the muscular process and the orbicularis apophysis is a deep notch for the chorda tympani nerve ("gct" in Fig. 18B). The osseous lamina (transversal lamina of Mason 2015) ("ol" in Figs. 18A–B) is a thin, triangular plate between the head, neck, manubrial base, and rostral process. The anterior free margin of the osseous lamina is thickened, creating a deep concavity on the lateral aspect of the osseous lamina. The rostral process often has raised edges (lamellae) on its inner (medial) and outer (lateral) margins (Henson 1961). The thick inner lamella extends from the head ("ila" in Fig. 18B), but as the rostral process is broken, it is unclear how far the inner lamella extends. Also, the inner lamella is often pierced by a foramen for the chorda tympani nerve (Henson 1961), which cannot be evaluated in the available brown rat sample. The outer lamella is most evident distally ("ola" in Fig. 15B). Between the two lamellae on the dorsal surface is the interlamellar sulcus for the chorda tympani nerve ("ils" in Fig. 15B).

The body of the incus ("bi" in Figs. 18C–D) has concave superior and inferior articular surfaces ("sas" and "ias," respectively, in Fig. 18D) contacting the articular facets on the malleus. Extending posteriorly from the body is the crus breve or short process ("cb" in Figs. 18C–D), which tapers to a blunt end that is held in the fossa incudis by the posterior incudal ligament. Perpendicular to the crus breve is the crus longum or long process ("cl" in Figs. 18C–D), which parallels the neck of the malleus in situ. At the distal end of the crus longum is the medially directed lenticular process ("lpr" in Figs. 18C–D), which contacts the stapes.

The stapes (Fig. 18E) is bicrurate with a large stapedial foramen (intercrural or obturator foramen) transmitting the proximal stapedial artery. The head of the stapes ("hs" in Fig. 18E), which articulates with the lenticular process of the incus, is not well delimited from the rest of the bone in

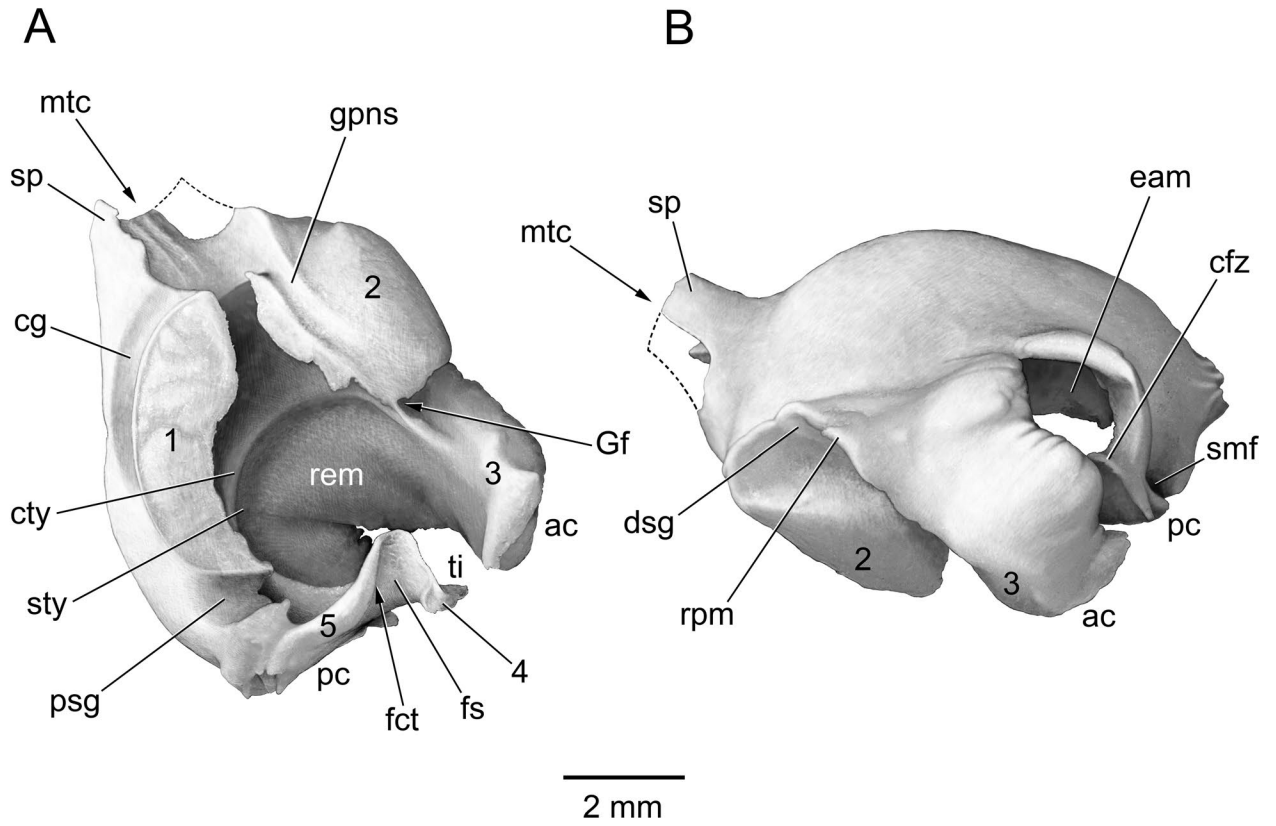

Fig. 17.—*Rattus norvegicus*, CM teaching collection, right ectotympanic with fused rostral process of the malleus. The damaged styliform process is reconstructed in dashed line based on the specimen's right side. **A,** ventral view, anterior to the top of the page; **B,** oblique posterolateral view, anterior to the left. Numbers 1-5 denote contact areas with the petrosal (see Fig. 6B): 1, rostral tympanic process; 2, epitympanic wing; 3, tegmen tympani; 4, tympanohyal; 5, caudal tympani process 1 + 2. Abbreviations: **ac,** anterior crus; **cfz,** chordaforsatz; **cg,** carotid groove; **cty,** crista tympanica; **dsg,** distal stapedial artery groove; **eam,** external acoustic meatus; **fct,** foramen for chorda tympani nerve (hidden); **fs,** facial sulcus; **Gf,** Glaserian fissure; **gpns,** greater petrosal nerve sulcus; **mtc,** musculotubal canal; **pc,** posterior crus; **psg,** proximal stapedial artery groove; **rem,** recessus meatus; **rpm,** rostral process of malleus (fused to ectotympanic); **smf,** position of stylomastoid foramen; **sp,** styliform process; **sty,** sulcus tympanicus; **ti,** tympanic incisure.

TTM M-2272, but has a more distinct rim in, for example, CM 10227 and 18604. The arrangement of the two crurae, anterior and posterior ("acr" and "pcr," respectively in Fig. 18E) is fairly symmetrical. Near the head, the posterior crus has a faint muscular process for the attachment of the stapedius muscle in TTM M-2272 ("mpr" in Fig. 18E); this is more distinct in, for example, CM 10227. The footplate, which occupies the fenestra vestibuli, has a slight thickened peripheral rim, the stapedial labrum, for the attachment of the annular ligament.

Neurovascular Structures

Nerves.—Branches of cranial nerves V, VII, and VIII are found in an around the petrosal and middle ear. Regarding the vestibulocochlear nerve (cranial nerve VIII), its branches are described above with the internal acoustic meatus in the dorsal view of the petrosal. Branches of the two other cranial nerves are considered below. Cranial nerve IX, the glossopharyngeal, often supplies the tympanic and lesser petrosal nerves in placentals (Davis and Story 1943; MacPhee 1981; Evans 1993), but Maynard and Downes (2019) reported these absent in the rat. Cranial nerve X, the vagus, often supplies the auricular branch in placentals, which joins the facial nerve at the stylomastoid foramen (Davis and Story 1943; MacPhee 1981; Evans 1993), but we have found no mention of this branch of the vagus in the rat literature.

The large sensory root and smaller motor root of the trigeminal nerve (cranial nerve V) run from the pons to the middle cranial fossa within a broad sulcus on the medial aspect of the crista petrosa ("trs" in Figs. 3, 14A; Greene 1935; Wysocki 2008). The only branch of the trigeminal nerve within the middle ear is the tensor tympani nerve. It enters the middle ear dorsal to the auditory tube (Berge and Wal 1990) through the musculotubal canal between the

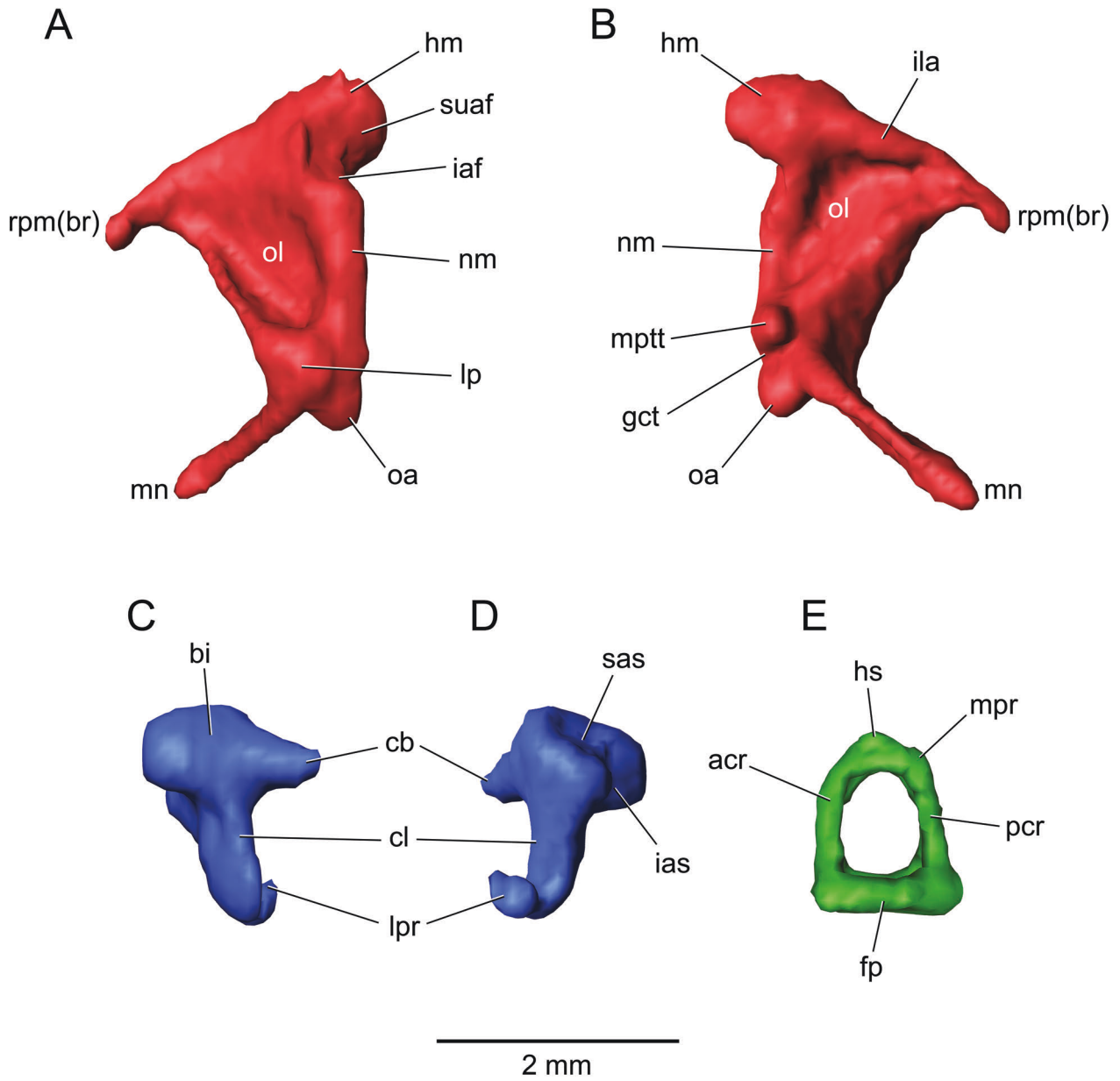

Fig. 18.—*Rattus norvegicus*, TTM M-2272, left auditory ossicles, isosurfaces rendered from CT data. **A,** malleus in lateral view, anterior to the left; **B,** malleus in medial view, anterior to the right; **C,** incus in lateral view, anterior to the left; **D,** incus in medial view, anterior to the right; **E,** stapes in ventral view, anterior to the left. Abbreviations: **acr,** anterior crus of stapes; **bi,** body of incus; **cb,** crus breve; **cl,** crus longum; **fp,** footplate of stapes; **gct,** groove for chorda tympani; **hm,** head of malleus; **hs,** head of stapes; **iaf,** inferior articular facet of malleus; **ias,** inferior articular surface of incus; **ila,** inner lamella; **lp,** lateral process of malleus; **lpr,** lenticular process; **mn,** manubrium; **mpr,** muscular process for stapedius muscle; **mptt,** muscular process for tensor tympani muscle; **nm,** neck of malleus; **oa,** orbicularis apophysis; **ol,** osseous lamina; **pcr,** posterior crus of stapes; **rpm(br),** broken rostral process of malleus; **sas,** superior articular surface of incus; **suaf,** superior articular facet of malleus.

ectotympanic and petrosal ("mtc" in Figs. 14A, 17). The nerve's course within the middle ear is not illustrated in the Figure 6C but it runs posterolaterally from the musculotubal canal and enters the muscle within the tensor tympani fossa ("ttf" in Fig. 6A) on the epitympanic wing.

Regarding the facial nerve (cranial nerve VII), Greene (1935) outlined the main branches; we include additional details based on the studied specimens. The facial nerve leaves the internal acoustic meatus via the facial canal in the foramen acusticum superius ("fc" in Fig. 9A). The facial canal leads to a space within the petrosal dorsal to the rear of the tensor tympani fossa (Fig. 6A). This space, the

cavum supracochleare, houses the geniculate ganglion of the facial nerve. Exiting the cavum supracochleare anteriorly via the hiatus Fallopii ("hF" in Fig. 6A) is the greater petrosal nerve ("gpn" in Fig. 6C). It leaves the ear region and joins the internal carotid nerve ("icn" in Fig. 6C) endocranially (Maynard and Downes 2019) to form the nerves of the pterygoid canal. The main trunk of the facial nerve leaves the geniculate ganglion in the posterior aspect of the cavum supracochleare via a broad aperture that represents the secondary facial foramen. Posterior to this, the facial nerve runs in company with (and dorsal to) the distal stapedial artery for a short stretch (Fig. 6C); initially the two are enclosed in bone and then in a partial canal formed by the crista parotica ("cp" in Fig. 6A). The distal stapedial artery turns medially at the fenestra vestibuli and the facial nerve continues posteriorly in the facial sulcus ("fs" in Fig. 6A), undercover of the tympanohyal ("th" in Fig. 6B). It is here that the facial nerve sends off the small stapedial nerve to the stapedius muscle (Berge and Wal 1990; not illustrated in Fig. 6C). The facial sulcus runs on the paroccipital process ("pp" in Fig. 6A) and exits the middle ear at the stylomastoid foramen between the petrosal and posterior crus of the ectotympanic ("smf" in Fig. 2). The posterior crus bears a sulcus transmitting the facial nerve from the foramen ("fs" in Fig. 17A). At the stylomastoid foramen, the facial nerve sends off the small chorda tympani nerve ("ctn" in Fig. 6C), which enters the middle ear via a tiny foramen in the posterior crus ("fct" in Fig. 17A). The chorda tympani runs on the dorsal surface of the mallear process of the posterior crus ("mp" in Figs. 11A, 12B, 17A). It passes medial to the malleus, within the notch between the muscular process for the tensor tympani and orbicularis apopohysis ("gct" in Fig. 18B). After crossing the osseous lamina, the chorda tympani exits the middle ear with the rostral process of the malleus via the Glaserian fissure (petrotympanic fissure of Greene 1935) between the tegmen tympani and anterior crus of the ectotympanic ("Gf" in Figs. 7A, 17A; "ctn" in Fig. 16). It is unknown if there is a separate foramen for the chorda tympani in the inner lamella on the rostral process of the malleus, as often occurs in placentals (Henson 1961).

Arteries.—The basicranial arteries have been described for *R. norvegicus* (Greene 1935; Guthrie 1963; Maynard and Downes 2019) and *R. rattus* (Tandler 1899). Based on these reports and the specimens studied, we reconstruct the main arteries onto the petrosal in ventral view (Fig. 6C).

The internal carotid artery is the primary artery of the basicranium and the major supplier of blood to the brain, with the vertebral arteries playing a secondary role (Guthrie 1963). Arising from the common carotid artery in the neck, the internal carotid artery divides into subequal branches as it approaches the posteromedial aspect of the auditory bulla. The anteriorly directed branch, the continuation of the internal carotid ("ica" in Fig. 6C), runs along the medial aspect of the bulla in a groove in the ectotympanic ("cg" in Figs. 14A, 17A) and then enters the carotid canal ("cc" in Fig. 1) between the ectotympanic, petrosal, and basioccipital. It is accompanied by the internal carotid nerve (deep petrosal nerve) (Maynard and Downes 2019; "icn" in Fig. 6C). The short carotid canal opens endocranially lateral to the low dorsum sellae ("ds" in Fig. 1) at the basisphenoid-basioccipital suture.

The laterally directed branch of the internal carotid is the stapedial artery (pterygopalatine artery of Greene 1935). As noted above, we divide the stapedial artery into a proximal part (from its internal carotid origin to the stapes; "psa" in Fig. 6C) and a distal part (from the stapes to its terminus at its end branches; "dsa" in Fig. 6C). The proximal stapedial artery enters the middle ear via the foramen between the pars cochlearis and ectotympanic in the posteromedial bullar wall ("psf" in Fig. 14A) and runs laterally across the promontorium in a groove ("psg" in Fig. 6A) near the anteroventral rim of the aperture of the cochlear fossula. It turns dorsally through the stapedial foramen in the stapes and then laterally and anteriorly accompanying the facial nerve as the distal stapedial artery (Fig. 6C). Although not reported by Tandler (1899), Greene (1935), Guthrie (1963), and Maynard and Downes (2019), a ramus posterior is described arising from the proximal stapedial artery medial to the fenestra vestibuli in several embryonic stages by Youssef (1966). As we found the dried artery in place in CM 17504, we have included the ramus posterior in our vascular reconstruction ("rp" in Fig. 6C). This branch ran posteriorly with the facial nerve and then out the stylomastoid foramen as the stylomastoid artery.

The common course of the facial nerve and distal stapedial artery is directed anteriorly, initially in a partial canal formed by the crista parotica ("cp" in Fig. 6A) and then into the substance of the petrosal bone in the facial canal. The nerve and artery diverge with the facial nerve continuing forward through the secondary facial foramen into the cavum supracochleare and the distal stapedial artery turning dorsolaterally, exiting the petrosal through the foramen for the distal stapedial artery on the cerebral surface of the petrosal ("dsf" in Figs. 8A, 10, 16). Endocranially, the distal stapedial artery runs in a groove on the dorsal surface of the ectotympanic ("dsg" in Figs. 16, 17B) and, according to Tandler (1899), divides into the smaller ramus superior and larger ramus inferior ("rs" and "ri," respectively in Fig. 6C). As noted by Wible (1987), an endocranial bifurcation for the superior and inferior rami is unusual among placentals. The ramus superior in the brown rat turns dorsally and supplies a meningeal branch and a small ramus temporalis exiting via a foramen in the squamosal ("frt" in Fig. 2). The ramus inferior runs anteriorly, exits the skull via the piriform fenestra, sends off a small artery of the pterygoid canal, and then enters the alisphenoid canal ("alc" in Figs. 2–3) en route to the orbit. The ramus inferior feeds the ramus infraorbitalis with the maxillary nerve, the ramus supraorbitalis with the ophthalmic nerve, and the ramus orbitalis with the optic nerve; the external carotid artery supplies the ramus mandibularis with the mandibular nerve.

Veins.—For our reconstruction of the veins on the petrosal (Figs. 9C, 13C), we follow the common pattern reported for the brown rat in Greene (1935), Butler (1967), and Szabó (1990, 1995). In addition, most of the relevant veins are dried in place and visible through the foramen magnum in CM 17504.

The large transverse sinus ("ts" in Fig. 13C) runs ventrally in the lateral margin of the tentorium cerebelli along the endocranial surface of the interparietal and supraoccipital ("ip" and "so," respectively in Fig. 3). As the transverse sinus approaches the petrosal, a small distributary, the superior (dorsal) petrosal sinus, runs anteromedially on the lateral aspect of the crista petrosa ("sps" in Figs. 9C, 13C) dorsal to the trigeminal nerve to connect with the cavernous sinus around the hypophysis. At the dorsolateral aspect of the subarcuate fossa, the transverse sinus divides into a larger postglenoid vein and a smaller sigmoid sinus ("pgv" and "ss," respectively in Figs. 9C, 13C). The postglenoid vein (transverse sinus of Greene 1935; petrosquamous sinus of Butler 1967 and Szabó 1990, 1995; retroglenoid vein of Maynard and Downes 2019) runs anteroventrally in a sulcus on the lateral surface of the pars canalicularis and then onto the lateral surface of the tegmen tympani (Fig. 13C). In lateral view in the skull, this part of the vein's course is covered by the overlying squamosal ("sq" in Fig. 2). The vein appears ventral to the squamosal through a gap between that bone and the tegmen tympani that represents the postglenoid foramen ("pgf" in Fig. 2).

From its origin, the sigmoid sinus ("ss" in Fig. 9C) runs posteromedially in a variably present sulcus posterior to the subarcuate fossa that reaches to the posteromedial aspect of the pars canalicularis. En route, the sigmoid sinus sends off the occipital emissary vein posteriorly ("oev" in Fig. 9C; occipital sinus of Butler 1967), which leaves the cranium via the mastoid foramen ("mf" in Figs. 2–3) between the petrosal and supraoccipital. At the posteromedial corner of the pars canalicularis, the sigmoid sinus divides with part exiting the foramen magnum into the vertebral veins ("vv" in Fig. 9C) and part joining the internal jugular vein ("ijv" in Fig. 9C). The main contributor to the internal jugular vein is the inferior (ventral) petrosal sinus ("ips" in Fig. 9C), which runs from the cavernous sinus in a sulcus on the medial aspect of the pars cochlearis ("ipss" in Fig. 14A). This sulcus faces the basioccipital, which encloses the inferior petrosal sinus in a partial canal (Fig. 1). CM 17504 shows that this partial canal is open endocranially and that the inferior petrosal sinus and small branch from the sigmoid sinus meet endocranially dorsal to the inferior jugular foramen to form the internal jugular vein.

COMPARISONS

We compare the petrosal and middle ear of the brown rat with those of several early and middle Eocene fossils to place the anatomy of the extant form in the context of the early members of the rodent lineage. Descriptions and illustrations of the ventral surface of the petrosal of several early and middle Eocene fossils have been published, notably the cocomyid *Cocomys lingchaensis* Li et al., 1989, from the early Eocene of China (Li et al. 1989; Wible et al. 2005) and the ischryomyoids *Paramys copei* Loomis, 1907, and *Paramys delicatus* Leidy, 1871, from the early and middle Eocene of the western United States, respectively (Wood 1962; Parent 1980; Wahlert 2000). While ectotympanics are not known for these three taxa, other Eocene fossils have been described with the ectotympanic bulla in place, notably the early Eocene cocomyid *Exmus mini* Wible et al., 2005, from China (Wible et al. 2005), the ischryomyoid *Reithroparamys delicatissimus* (Leidy, 1871) (Wood 1962; Meng 1990), and the sciuravid *Sciuravus nitidus* Marsh, 1871 (Dawson 1961; Parent 1980; Wahlert 2000), both from the middle Eocene of the western United States. The middle ear anatomy of these Eocene fossils is not uniform, but as noted below, there are numerous shared similarities. Descriptions and illustrations of the dorsal view of the petrosal in these fossils are lacking in the literature, which we amend here based on the CT scans of *Paramys delicatus*, AMNH 12506.

The phylogenetic position of the Eocene fossils sampled here is controversial. In some phylogenetic analyses, *Cocomys* Li et al., 1989, *Paramys* Leidy, 1871, *Reithroparamys* Matthew, 1920, and *Sciuravus* Marsh, 1871, fall outside of the rodent crown group (Meng et al. 2003: figs. 74–75; Asher et al. 2005), whereas in others (Marivaux et al. 2004) *Paramys* and *Reithroparamys* are within crown Rodentia, but *Cocomys* is not. The position of *Exmus* Wible et al., 2005, has not yet been similarly tested. Using a node-based definition, Wyss and Meng (1996) proposed Rodentiaformes to include the stem and crown Rodentia. Consequently, applying that definition, the Eocene fossils sampled here are rodentiaforms in some analyses (Meng et al. 2003; Asher et al. 2005), but in others (Marivaux et al. 2004) some fossils are rodents and others rodentiaforms. For ease of description here, we refer to our entire fossil sample as rodents with the caveat that this controversy is still unresolved.

Petrosal

Ventral view.—A major distinction between the brown rat and the Eocene rodents is that the petrosal of the former is more loosely held in the cranium (Figs. 1–3). Anteriorly and anterolaterally, the large piriform fenestra separates the petrosal from the basisphenoid, alisphenoid, and squamosal; medially and posterolaterally, the petrosal has minimal contacts with the basioccipital and squamosal, respectively; it is only posteriorly where the petrosal is held fast to the ex- and supraoccipital. Although a piriform fenestra is found throughout our Eocene rodent sample, its size varies from being restricted anterolaterally in *Cocomys* (Li et al. 1989; Wible et al. 2005) to present across the entire anterior aspect of the petrosal in *Paramys delicatus*

(Fig. 19). Nevertheless, the petrosal is more tightly held in the cranium along its other borders in the Eocene sample than in the brown rat. In *Paramys delicatus*, for example, the entire medial aspect of the petrosal is tightly bound to the basioccipital and its tympanic process (Fig. 19); laterally, the petrosal is overlapped broadly by the squamosal (Figs. 20). Additionally, although not visible in ventral view, the petrosal is also buttressed endocranially by the tentorial process of the parietal ("tpa" in Figs. 20–21).

The brown rat and the Eocene rodents considered here have a shelf medial to the promontorium, which is angled ventromedially to abut the basioccipital. In the brown rat, this shelf has a concave surface that provides broad support for the ectotympanic bulla ("1" in Fig. 22B) and is identified here as the rostral tympanic process (Fig. 5). Where this surface is visible in the Eocene sample, it is flatter (e.g., *Cocomys*, Wible et al. 2005: fig. 7A; Figs. 19, 22A), but still has been interpreted as contacting the ectotympanic, based on extant rodents and other fossils with the bulla in place (e.g., *Reithroparamys*, Meng 1994; Wahlert 2000; *Exmus*, Wible et al. 2005). Wible et al. (2005) called this structure the anteromedial shelf in Eocene rodents, but given the extent to which this shelf is angled ventrally into the medial wall of the middle ear, it is better identified as the rostral tympanic process.

The brown rat and the Eocene sample have an epitympanic wing that is continuous with the rostral tympanic process (Fig. 22). This surface includes a concavity for the origin of the tensor tympani muscle as well as the aperture for the hiatus Fallopii. The Eocene sample differs from the brown rat in that the fossils have a high septum extending anteriorly from the anterolateral aspect of the promontorium that delimits the epitympanic wing medially and defines a deep groove for the internal carotid artery laterally ("icg" in Fig. 22A); the brown rat has a low septum in a comparable place and no groove for the internal carotid (Fig. 22B). Further distinguishing the brown rat is its oblique septum on the epitympanic wing delimiting a posteromedial space for the tensor tympani from an anterolateral space for the ectotympanic ("2" in Fig. 22B); such a septum is lacking in the Eocene sample. The precise relationship between the epitympanic wing and ectotympanic in the Eocene rodents has not been described. However, if contact occurred, it was not on the same scale as in the brown rat as a sizeable facet is not found in the fossils; we designate a possible small area of contact on the epitympanic wing in *Paramys delicatus* ("2" in Fig. 22A).

The brown rat and the Eocene sample have a tegmen tympani that at its anterior end tapers into a ventrally inclined process (Figs. 13A, 20, 22). Posteriorly on the tegmen tympani is the epitympanic recess (Fig. 22), which includes the fossa incudis in its posterior margin (Figs. 6A). In both the brown rat and Eocene sample, the fossa incudis is poorly delimited from the epitympanic recess and the tegmen tympani forms the lateral wall for the two spaces; in many placentals, the squamosal contributes to this lateral wall (Wible 2008, 2009, 2010; Wible and Spaulding 2013). The Eocene sample differs in having a more confined space for the epitympanic recess (Fig. 22). In the brown rat, the tegmen tympani also provides attachment for the anterior crus of the ectotympanic anteriorly and along its lateral margin ("3" in Figs. 6B, 22B). Based on Meng (1994: fig. 2), *Reithroparamys* has a similar contact between the tegmen tympani and anterior crus. The epitympanic recess and the surface contacting the ectotympanic are not demarcated but appear continuous in the brown rat (Fig. 22B). In contrast, in *Paramys copei* (Wahlert 2000) and *Paramys delicatus* (Fig. 22A), two distinct surfaces delimited by a low, subtle ridge are found on the tegmen tympani: a posterior one for the epitympanic recess and an anterior one for the ectotympanic, the latter was called the bullar process of the petrosal by Wahlert (2000). *Cocomys* (Wible et al. 2005: fig. 7) resembles the brown rat in that only one continuous surface is present on the tegmen tympani. Wible et al. (2005: fig. 7B) erroneously placed their label for the epitympanic recess ("er") in *Cocomys* in the anterior part of the tegmen tympani; it should have been located more posteriorly and not in the surface that likely contacted the ectotympanic. A major distinction between the brown rat and the Eocene sample concerns the relationship between the tegmen tympani and epitympanic wing; whereas these structures have a broad abutment in the Eocene petrosals (Fig. 22A; Wible et al. 2005), they are widely separated in the brown rat (Fig. 22B).

On the ventral surface of the pars canalicularis, the brown rat has a tripartite caudal tympanic process (Figs. 6A–B, 22B): parts one and two are continuous, form a low curved ridge on a raised platform behind the aperture of the cochlear fossula, and contact the posterior crus of the ectotympanic; part three, which is separated from the other parts, lies more posteriorly, forms a high wall between the paroccipital process and paracondylar process of the exoccipital, and does not contact the ectotympanic. In contrast, *Cocomys* (Wible et al. 2005: fig. 7), *Paramys copei* (Wahlert 2000: fig. 2), and *Paramys delicatus* (Fig. 22A) have very little in the way of caudal tympanic processes. There is a raised platform behind the aperture of the cochlear fossula that likely contacted the posterior crus of the ectotympanic ("5" in Fig. 22A), based on *Exmus* (Wible et al. 2005: fig. 8) and *Reithroparamys* (Meng 1990: fig. 1), but there is little elevation on this platform. In the brown rat this platform has a distinct depression, the cochlear fossula, but this is lacking in the Eocene sample. Also, there is no ridge connecting the paroccipital process and paracondylar process of the exoccipital in the Eocene sample, which means there is no petrosal wall defining the rear of the middle ear space.

In the brown rat, the course of the facial nerve through the middle ear is hidden in ventral view by the tympanohyal and the crista parotica (Fig. 23B). In contrast, in *Paramys delicatus* (Fig. 23A), *Paramys copei* (Wahlert 2000: fig. 3), and *Cocomys* (Wible et al. 2005: figs. 7A–B), the facial nerve runs open in a facial sulcus posterior to the secondary facial foramen, which lies anterior to the fenestra

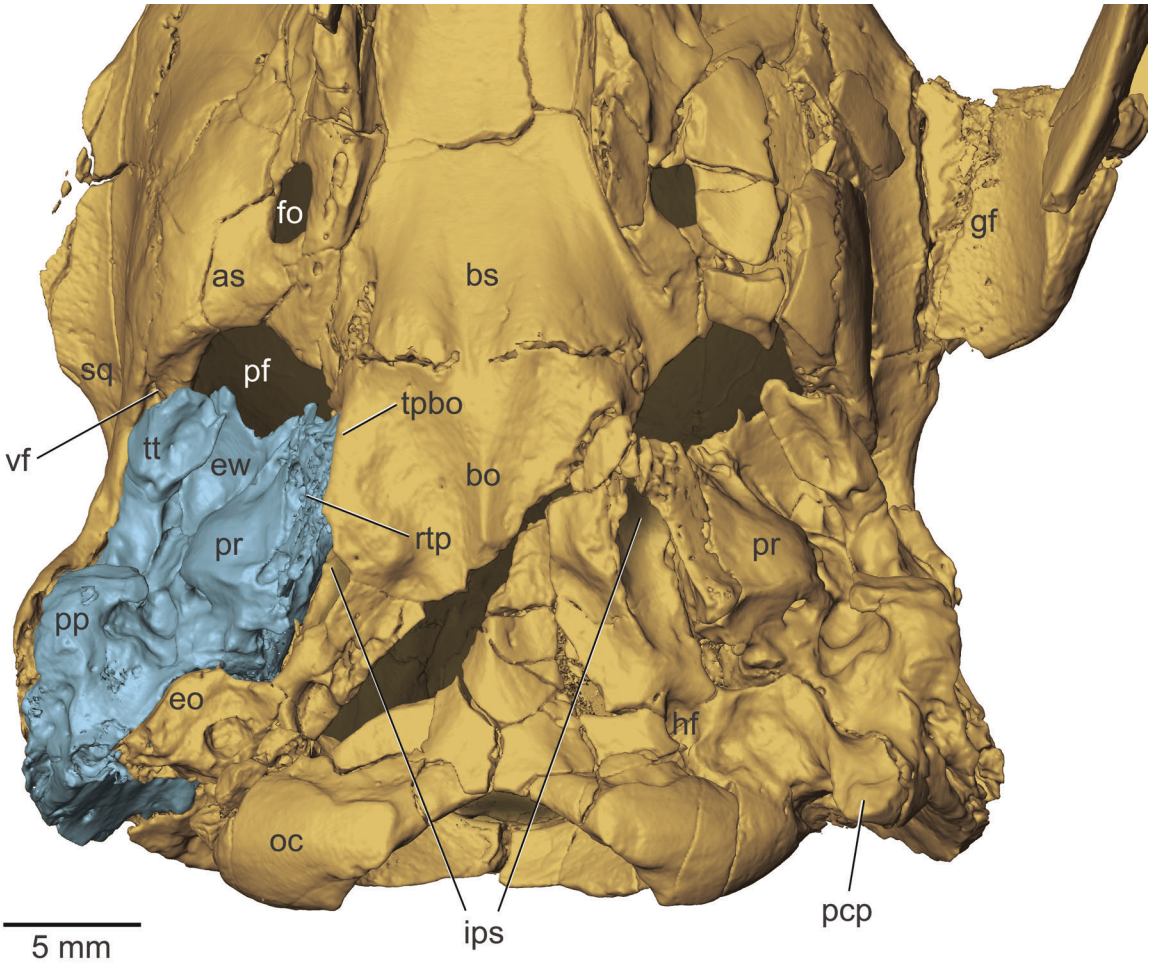

Fig. 19.—*Paramys delicatus*, AMNH 12506, basicranium, isosurface rendered from CT data in ventral view anterior to the top. Right petrosal in light blue. Specimen has multiple cracks, including a sizeable oblique one across the basioccipital; the canal for the inferior petrosal sinus is broken open on the left side, the paracondylar process of the exoccipital is broken on the right side, and the right rostral tympanic process of the petrosal has a mangled surface whereas the left is smooth. Abbreviations: **as,** alisphenoid; **bo,** basioccipital; **bs,** basisphenoid; **eo,** exoccipital; **ew,** epitympanic wing of petrosal; **fo,** foramen ovale; **gf,** glenoid fossa; **hf,** hypoglossal foramen; **ips,** canal for inferior petrosal sinus; **pcp,** paracondylar process of exoccipital; **pf,** piriform fenestra; **pp,** paroccipital process of petrosal; **pr,** promontorium of petrosal; **rtp,** rostral tympanic process of petrosal; **sq,** sqamosal; **tpbo,** tympanic process of basioccipital; **tt,** tegmen tympani; **vf,** venous foramen to the right.

vestibuli. The tympanohyal in the Eocene sample is a medially directed, rounded process in *Paramys delicatus* (Fig. 22A), *Paramys copei* (labeled mastoid eminence in Wahlert 2000: fig. 1), and *Cocomys* (Wible et al. 2005: figs. 7A–B), whereas in the brown rat it is pointed and posteromedially directed (Fig. 6B). The posterior crus of the ectotympanic is fused to the tympanohyal in the brown rat ("4" in Fig. 6B). In *Paramys delicatus*, the anterior surface of the tympanohyal has a depression that we interpret as contacting the posterior crus ("4" in Fig. 22A). We are uncertain if this facet occurs in *Cocomys* and *Paramys copei*, but Wible et al. (2005) reported the posterior crus abutting the base of the tympanohyal in *Exmus*.

Dorsal view.—Among Eocene rodents, our comparisons in this view are limited to *Paramys delicatus* (Figs. 21, 24A). In both *Paramys delicatus* (Fig. 21) and the brown rat (Fig. 3), the width of the internal acoustic meatus and subarcuate fossa are roughly subequal as are the overall orientations of these apertures in the cranium. A major difference in the internal acoustic meatus is its depth: in the brown rat (Figs. 8A, 9) the transverse crest is little recessed from the surrounding surface, which makes the meatus shallow, whereas in *Paramys delicatus* (Figs. 21, 24A) the transverse crest is deeply recessed, which makes the meatus deep. On the pars cochlearis, a major difference highlighted in dorsal view is the large exposure of the dorsal surface of the rostral tympanic process in

Paramys delicatus (Fig. 24A), which is directed ventromedially to abut the tympanic process of the basioccipital (Figs. 19–20); in the brown rat the rostral tympanic process is more ventrally directed (Figs. 3, 14A). In both taxa the dorsal surface of the rostral tympanic process contributes to the passageway for the inferior petrosal sinus (Figs. 6C, 14A, 19, 24). Another similarity on the pars cochlearis is the position of the cochlear canaliculus, which is recessed dorsally from the jugular foramen in both (Figs. 14A, 21).

Along the lateral aspect of the petrosal, the brown rat has a high crista petrosa that runs the length of the pars cochlearis and pars canalicularis (Fig. 24B), whereas in *Paramys delicatus* the crista petrosa is only developed on the pars canalicularis (Fig. 24A). The crista petrosa in the brown rat does not contact other bones (Fig. 3), but in *Paramys delicatus* anteriorly it is sutured to a robust tentorial process of the parietal ("tpa" in Figs. 20, 21) and also has a small contact lateral to that with the squamosal. As noted with the ventral view, the brown rat tegmen tympani in the dorsal view is widely separated from the pars cochlearis (Fig. 24B) with the foramen for the distal stapedial artery situated in the depth of the separating gap (Figs. 8A, 10, 24B). The space between the crista petrosa and the tegmen tympani includes a broad cerebral surface in the brown rat (Figs. 8A, 10). In contrast, the tegmen tympani in *Paramys delicatus* is not separated by a gap (Fig. 24A); its dorsal roof does not contribute to the cerebral surface but is overlain by the squamosal. There is a small cerebral surface on the roof of the epitympanic wing ("cs" in Fig. 24A).

A last striking difference is in the size of the sigmoid sinus sulcus, which is dramatically broader in *Paramys delicatus* in comparison to the brown rat (Fig. 24), which is variably present (Fig. 10). Additionally, most of the outflow from the sigmoid sinus in the brown rat was directed through the foramen magnum (Fig. 9C), whereas the jugular foramen was the primary conduit in *Paramys delicatus* (Figs. 21, 23A).

Lateral view.—In the brown rat (Fig. 2), *Paramys delicatus* (Fig. 20), *Cocomys* (Wible et al. 2005: figs. 7A–B), and *Exmus* (Wible et al. 2005: Fig. 3), the tegmen tympani is visible in direct lateral view in the cranium. This also appears to be the case in *Reithroparamys* (Meng 1990: fig. 2). However, the exposure is more significant in the brown rat, given that the squamosal barely contacts the petrosal here and the piriform fenestra expands into the gap between these two bones (Fig. 2).

Ectotympanic, Malleus, Incus, and Stapes

The expanded ectotympanic of the brown rat is tightly coupled to the petrosal, with five points of contact around the circumference of the ectotympanic abutting surfaces on the pars cochlearis and pars canalicularis and fusing to the tympanohyal (Figs. 6B, 17); the anterior crus of the ectotympanic also has a point contact with the squamosal (Fig. 2). Ectotympanics have been reported for some early and middle Eocene rodents, such as *Sciuravus nitidus* (Dawson 1961; Wahlert 2000), *Reithroparamys delicatissimus* (Meng 1990), and *Exmus mini* (Wible et al. 2005). In *Sciuravus*, Dawson (1961) recorded the ectotympanic present and on one side only in two of seven specimens, suggesting to her that this element must be only loosely attached. In *Reithroparamys* (Meng 1991) and *Exmus* (Wible et al. 2005), the ectotympanic is reported to be more firmly attached. Of these three extinct forms, the most detail on the contacts of the ectotympanic are provided for *Exmus* by Wible et al. (2005). It has five points of contact on the petrosal comparable to those in the brown rat, although that on the epitympanic wing is not bulbous or as large as in the brown rat ("2" in Fig. 17). Along with the petrosal, the ectotympanic in *Exmus* broadly contacts the posttympanic process of the squamosal, the entoglenoid process of the squamosal, the ectopterygoid crest of the alisphenoid, and the tympanic process of the basioccipital. Ectotympanics have not been reported for *Paramys delicatus*, *Paramys copei*, and *Cocomys lingchaensis*, suggesting that this bone must have been loosely attached. As noted above, the petrosal of *Paramys delicatus* appears to have five points of contact for the ectotympanic (Fig. 22A) in positions comparable to those in the brown rat (Fig. 22B). Another similarity regarding the ectotympanic is the chordafortsatz ("cfz" in Figs. 11A, 12B, 17A); Wible et al. (2005:115) described the same process on the posterior crus of the ectotympanic in *Exmus*. A foramen for the chorda tympani nerve in the posterior crus is not reported for *Exmus*, but this may be an oversight due to preservation.

The brown rat malleus is fused to the ectotympanic through its elongate rostral process (Figs. 15B, 16) and has a small orbicular apophysis, making it a microtype malleus of Fleischer (1978; Mason 2013; in contrast to the freely mobile type). The only malleus reported for an early Eocene rodent is that of *Exmus*, a left malleus (missing the rostral process) in articulation with the incus (Wible et al. 2005). The left incus of *Exmus* is very similar to that of the brown rat in the proportions of the crus longum and crus breve. What is preserved of the malleus in *Exmus* is remarkably like the brown rat malleus, with an elongate neck and expanded osseous lamina (Figs. 15A–B); the most significant difference is the absence of any orbicular apopohysis in *Exmus*. This absence puts the malleus of *Exmus* into the therian ancestral type (Fleischer 1978; Mason 2013). The addition of the orbicular apophysis, as in the brown rat, characterizes the microtype, which is associated with species hearing higher-frequencies.

Neurovascular Structures

Nerves.—Comparisons between the brown rat and our Eocene sample regarding the facial nerve are included with the petrosal above. This is the only nerve on the petrosal that has been reported for our Eocene sample (Wahlert

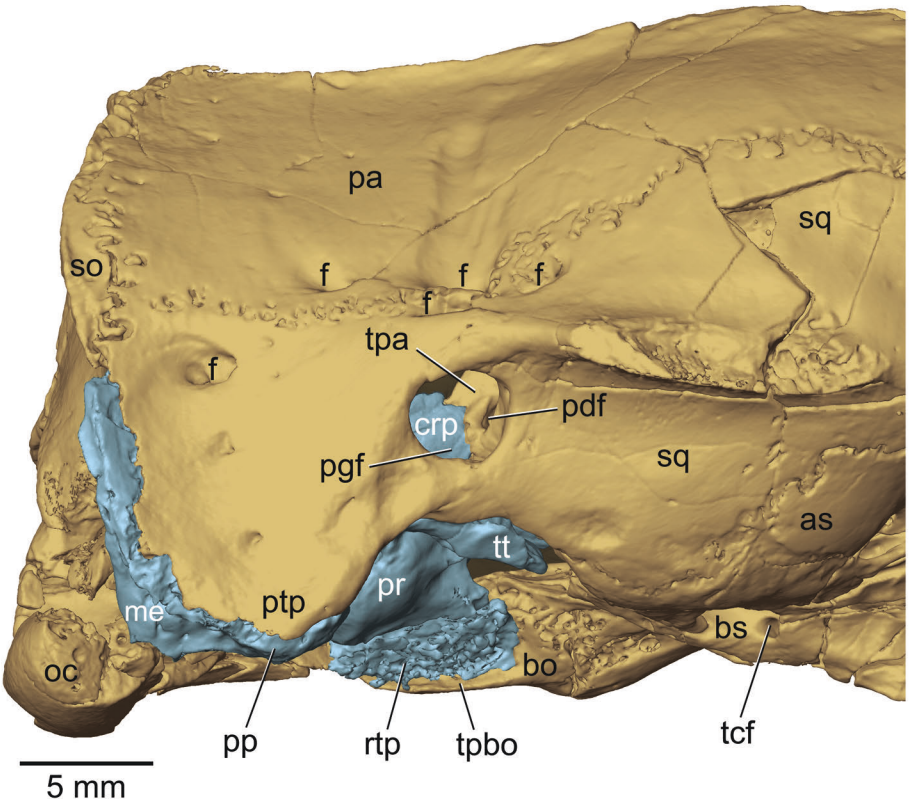

Fig. 20.—*Paramys delicatus*, AMNH 12506, right posterior braincase, isosurface rendered from CT data in lateral view anterior to the right. Right petrosal in light blue. The paracondylar process of the exoccipital and the zygomatic process of squamosal are broken on the right side; the surface of the right rostral tympanic process of the petrosal has a mangled surface. Abbreviations: **as,** alisphenoid; **bo,** basioccipital; **bs,** basisphenoid; **crp,** crista petrosa; **f,** ramus temporalis foramen; **me,** mastoid exposure; **oc,** occipital condyle; **pa,** parietal; **pdf,** posterior division foramen; **pgf,** postglenoid foramen; **pp,** paroccipital process of petrosal; **pr,** promontorium of petrosal; **ptp,** posttympanic process of squamosal; **rtp,** rostral tympanic process of petrosal; **so,** supraoccipital; **sq,** sqamosal; **tcf,** transverse canal foramen; **tpa,** tentorial process of parietal; **tpbo,** tympanic process of basioccipital; **tt,** tegmen tympani.

2000; Wible et al. 2005) and leaves impressions on the *Paramys delicatus*, AMNH 12506, studied here.

Arteries.—The internal carotid artery in the brown rat follows an extracranial course medial to the bulla and then into the cranial cavity through a short carotid canal between the basioccipital, petrosal, and ectotympanic (Figs. 1, 23B), a perbullar course (Wible 1986). In contrast, *Paramys delicatus* (Fig. 22A), *Paramys copei* (Wahlert 2000), *Cocomys* (Wible et al. 2005), and *Sciuravus* (Wahlert 2000) have grooves ("icg" in Fig. 22A) indicating a transpromontorial course for the internal carotid (Wible 1986; Fig. 23A). In *Paramys delicatus* (Fig. 22A), a short groove at the posteromedial aspect of the pars cochlearis marks the internal carotid's entrance into the middle ear, and at the anterior pole of the promontorium, the prominent septum on the medial aspect of the epitympanic wing noted above marks the lateral margin of a well-developed carotid groove near the artery's exit from the middle ear. Between these two grooves, the promontorial surface is smooth. *Cocomys* (Wible et al. 2005: fig. 7) and *Paramys copei* (Wahlert 2000: fig. 2) have only the anterior of these two grooves, but *Sciuravus* has a continuous transpromontorial groove crossing the promontorium (Wahlert 2000: fig. 4). Regarding the entrance of the artery into the cranial cavity, *Paramys copei* (Wahlert 2000), *Cocomys* (Wible et al. 2005), and *Sciuravus* (Wahlert 2000) have a carotid foramen enclosed between the petrosal and sphenoid, close to the juncture of the basi- and alisphenoid, but *Paramys delicatus* lacks a separate carotid foramen and the artery entered the cranial cavity via the large piriform fenestra (Fig. 19). Wible et al. (2005) noted the course of the internal carotid in *Exmus* was not entirely clear but suggested based on a small aperture in the medial bullar wall that it followed a perbullar course as described here for the brown rat. *Reithroparamys* appears to lack the segment of the internal carotid artery that in the other taxa enters the cranial cavity to supply the brain (Meng 1990).

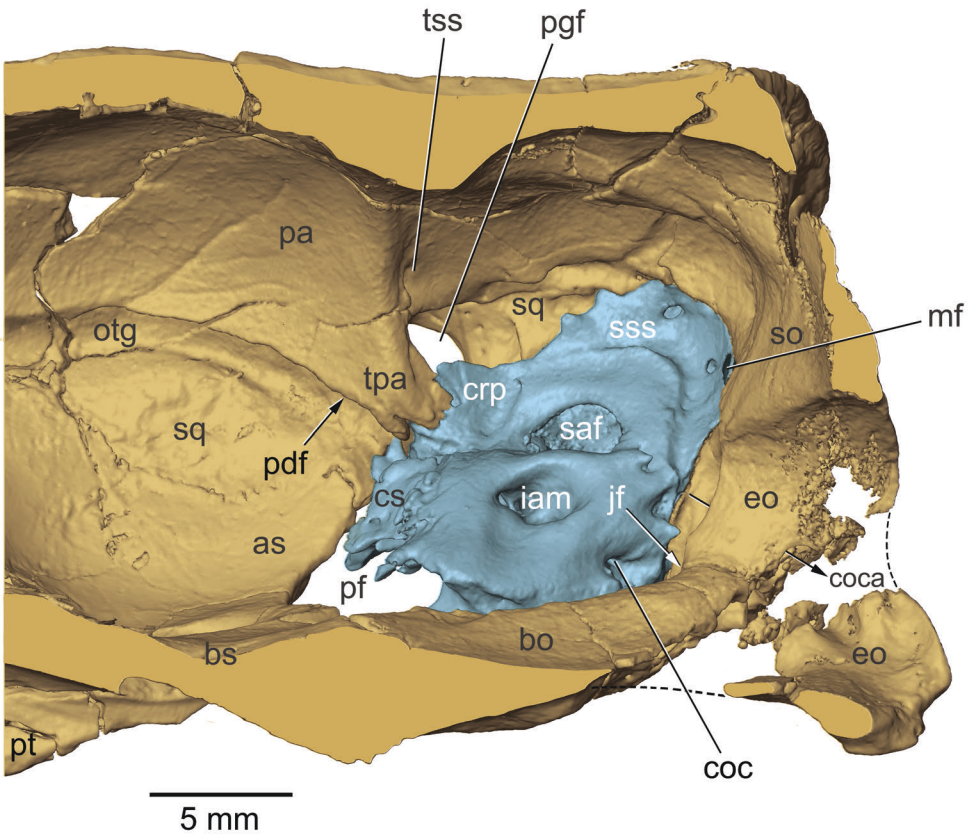

Fig. 21.—*Paramys delicatus*, AMNH 12506, right posterior braincase, isosurface rendered from CT data in medial view, anterior to the left. Right petrosal in light blue. The right exoccipital is damaged and dashed lines show the outline based on the left side. For simplification, the spongy bone along the cut midline edge has been filled in with uniform color. Abbreviations: **as,** alisphenoid; **bo,** basioccipital; **bs,** basisphenoid; **coc,** cochlear canaliculus; **coca,** condyloid canal; **crp,** crista petrosa; **cs,** cerebral surface; **eo,** exoccipital; **iam,** internal acoustic meatus; **jf,** jugular foramen; **mf,** mastoid foramen; **otg,** orbitotemporal groove; **pa,** parietal; **pdf,** posterior division foramen; **pf,** piriform fenestra; **pgf,** postglenoid foramen; **pt,** pterygoid; **saf,** subarcuate fossa; **so,** supraoccipital; **sq,** sqamosal; **sss,** sigmoid sinus sulcus; **tpa,** tentorial process of parietal; **tss,** transverse sinus sulcus.

The proximal stapedial artery is the main branch of the internal carotid in the brown rat where it arises outside the middle ear and has its own foramen of entrance into that space (Figs. 14A, 23B). In contrast, in *Paramys delicatus* (Figs. 22A, 23A), *Paramys copei* (Wahlert 2000: fig. 2), *Cocomys* (Wible et al. 2005: fig. 7), and *Sciuravus* (Wahlert 2000: fig. 4), the proximal stapedial arises on the promontorium within the middle ear. The arterial pattern differs in *Reithroparamys*, which appears to only have a proximal stapedial artery and no internal carotid entering the cranial cavity (Meng 1990) as reported, for example, in extant *Sciurus* (Tandler 1899; Guthrie 1963). It also differs in *Exmus*, which has an extratympanic origin for the proximal stapedial (Wible et al. 2005) as in the brown rat. Based on the size of the carotid canal and proximal stapedial artery groove in the brown rat, its internal carotid and proximal stapedial arteries appear subequal (Fig. 23B). However, judging from the size of the grooves on the promontorium in *Paramys delicatus* (which is only present at the fenestra vestibuli and not really visible in Fig. 22A), *Paramys copei* (Wahlert 2000: fig. 2), and *Cocomys* (Wible et al. 2005: figs. 7A–B), the internal carotid is the larger of the two vessels (Fig. 23A); the reverse is the case in *Sciuravus* (Wahlert 2000: fig. 4) and *Exmus* (Wible et al. 2005). At the lateral edge of the promontorium, the brown rat proximal stapedial artery sends off a ramus posterior (Fig. 23B) without any bony indication of the vessel's presence. The occurrence of a ramus posterior in the fossils cannot be confirmed or denied and is not included in our reconstruction of *Paramys delicatus* (Fig. 23A).

Lateral to the fenestra vestibuli, the distal stapedial artery in the brown rat turns anteriorly with the facial nerve undercover of the crista parotica (Fig. 23B). The two become enclosed in a short canal, with the facial nerve then entering the cavum supracochleare and the distal stapedial artery reaching the endocranial surface, exiting the petrosal at a foramen in the gap between the tegmen tympani and epitympanic wing (Figs. 8A, 10, 16, 24B). At this

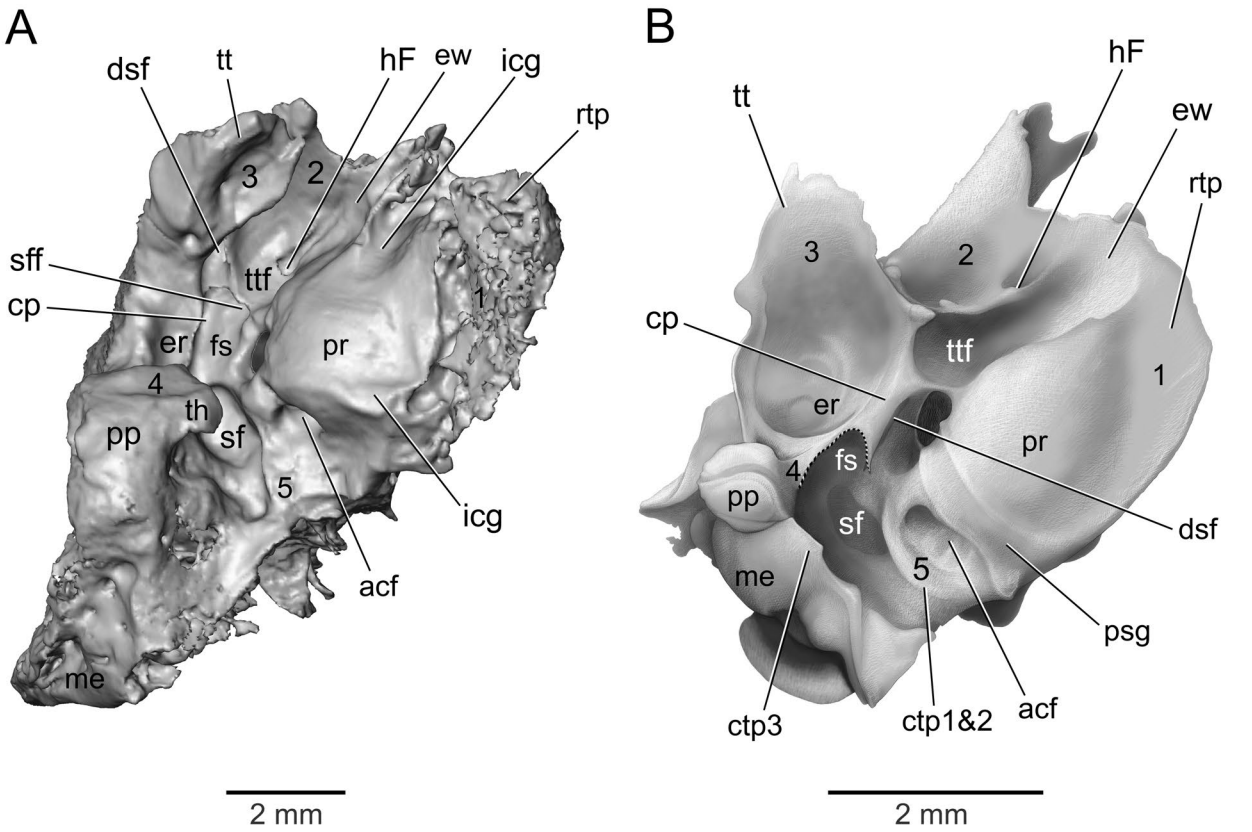

Fig. 22.—Right petrosals in ventral view, anterior to the top of the page. **A,** *Paramys delicatus*, AMNH 12506, isosurface rendered from CT data; **B,** *Rattus norvegicus*, CM teaching collection (see Fig. 6A). Numbers 1 to 5 are surfaces contacting the ectotympanic (see Figs. 6B, 17). In A, the surface of the rostral tympanic process is mangled; in A, the tympanohyal is broken, with the break indicated by dotted line. Abbreviations: **acf,** aperture of cochlear fossula; **cp,** crista parotica; **ctp1&2,** part 1 and 2 of caudal tympanic process (see Fig. 5B); **ctp3,** part 3 of caudal tympanic process (see Fig. 5B); **dsf,** distal stapedial artery foramen; **er,** epitympanic recess; **ew,** epitympanic wing; **fs,** facial sulcus; **hF,** hiatus Fallopii; **icg,** internal carotid groove; **me,** mastoid exposure; **pp,** paroccipital process; **pr,** promontorium; **psg,** proximal stapedial artery groove; **rtp,** rostral tympanic process; **sf,** stapedius fossa; **sff,** secondary facial foramen; **th,** tympanohyal; **tt,** tegmen tympani; **ttf,** tensor tympani fossa.

point, the distal stapedial artery branches into a large ramus inferior that exits the piriform fenestra and a small ramus superior that supplies the meninges and a ramus temporalis (Fig. 23B), equivalent to the posterior division of the ramus superior (Rougier and Wible 2006). Lateral to the fenestra vestibuli in *Paramys delicatus* (Fig. 23A), *Paramys copei* (Wahlert 2000: figs. 1–3), and *Cocomys* (Wible et al. 2005: fig. 7), the distal stapedial artery runs anteriorly with the facial nerve in the open facial sulcus. The two diverge, with the facial nerve entering the secondary facial foramen and the distal stapedial artery entering a foramen near the juncture of the tegmen tympani and epitympanic wing ("dsf" in Fig. 22A). The further course of the distal stapedial artery is only known fully in *Paramys delicatus* through the CT scan data. The artery appears on the endocranial surface in the seam between the tegmen tympanic and epitympanic wing ("dsf" in Fig. 24A). The bulk of the artery moves forward as the ramus superior into a broad orbitotemporal groove on the squamosal ("otg" in Fig. 20). However, there is a passageway between the tegmen tympani and epitympanic wing (not visible in the figures) for a small ramus inferior ("ri" in Fig. 23A), which would have exited the cranium by the piriform fenestra. Soon after entering the orbitotemporal groove, the ramus superior divides into anterior and posterior divisions ("ad" and "pd," respectively in Fig. 23A). The large anterior division runs forward to the orbit in the orbitotemporal groove; the smaller posterior division passes posterodorsally into a foramen between the tentorial process of the parietal and the overlying squamosal ("pdf" in Figs. 20–21). This foramen opens into a wide space just internal to the postglenoid foramen ("pgf" in Fig. 20), where the posterior division branches into rami temporales, which exit the skull via five large foramina near the parietosquamous suture ("f" in Fig. 20). The number of foramina for rami temporales (temporal foramen of Hill 1935) varies in the Eocene sample, for example, with two in *Exmus* (Wible et al. 2005) and *Sciuravus* (Wahlert 1974), two on the left and three on the right in *Cocomys* (Wible et al. 2005), and three in *Paramys copei* (Wahlert

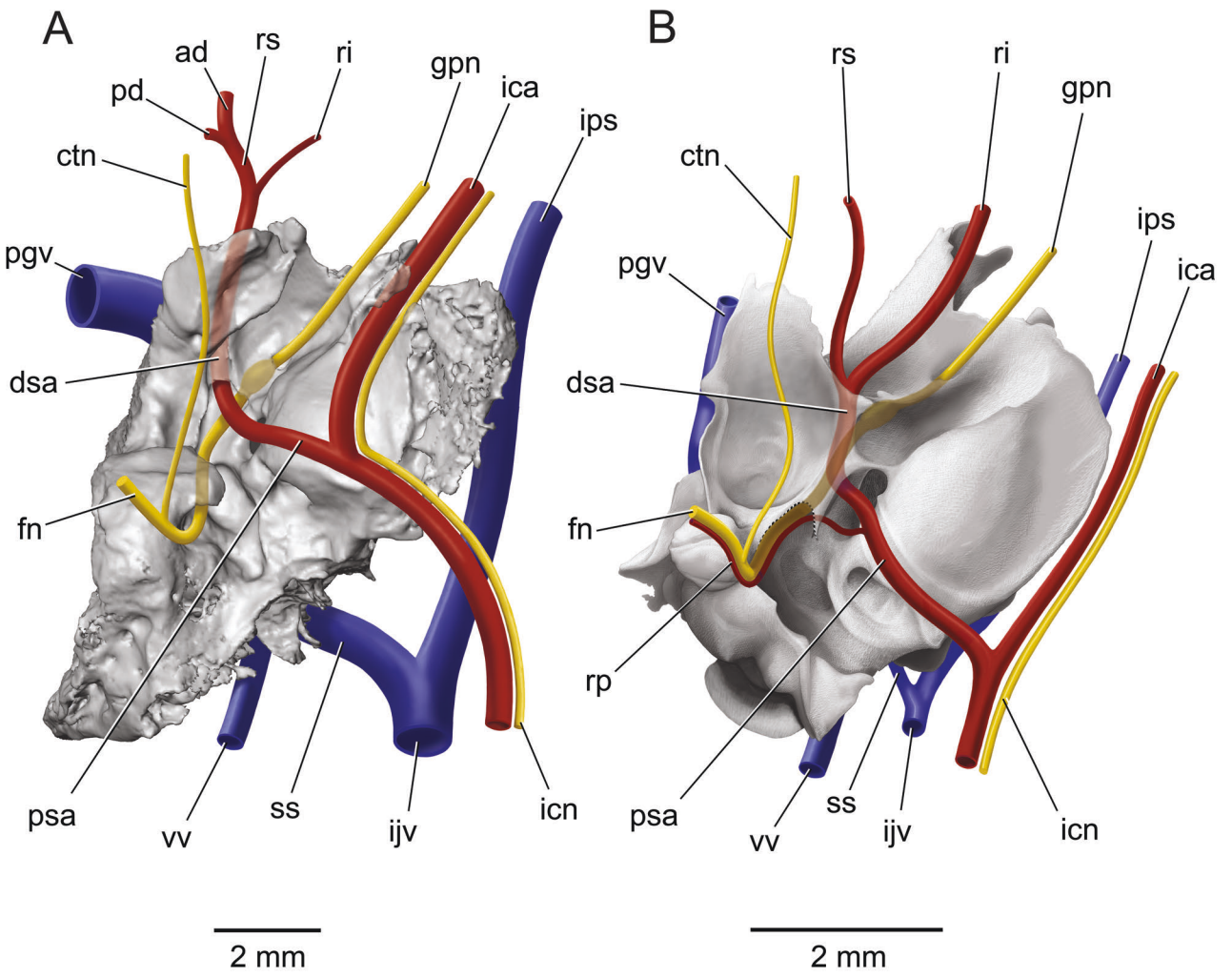

Fig. 23.—Right petrosals in ventral view, with nerves, arteries, and veins reconstructed, anterior to the top of the page. **A,** *Paramys delicatus*, AMNH 12506, isosurface rendered from CT data (see Fig. 22A); **B,** *Rattus norvegicus*, CM teaching collection (see Fig. 6C). Abbreviations: **ad,** anterior division of ramus superior; **ctn,** chorda tympanic nerve; **dsa,** distal stapedial artery; **fn,** facial nerve; **gpn,** greater petrosal nerve; **ica,** internal carotid artery; **icn,** internal carotid nerve; **ijv,** internal jugular vein; **ips,** inferior petrosal sinus; **pd,** posterior division of ramus superior; **pgv,** postglenoid vein; **psa,** proximal stapedial artery; **ri,** ramus inferior; **rp,** ramus posterior; **rs,** ramus superior; **ss,** sigmoid sinus; **vv,** vertebral vein.

1974). Another specimen of *Paramys delicatus*, USNM 23556, is illustrated by Wahlert (1974: fig. 3) with only two.

In summary, *Paramys delicatus* has a basicranial arterial pattern resembling that thought to be primitive for Eutheria (Wible 1987; Rougier and Wible 2006; O'Leary et al. 2013), with a transpromontorial internal carotid and a stapedial artery dividing into ramus inferior and ramus superior, which in turn divides into anterior and posterior divisions. The pattern of *Paramys delicatus* differs from the primitive one regarding the location of the stapedial artery bifurcation into ramus inferior and ramus superior; it is within the endocranium in *Paramys delicatus* rather than within the middle ear. The brown rat deviates from the primitive eutherian pattern with a perbullar internal carotid, an extratympanic origin for the proximal stapedial artery, an endocranial origin of the ramus inferior and ramus superior, and the absence of the anterior division of the ramus superior. Not all Eocene taxa exhibit the same pattern as *Paramys delicatus*; *Exmus* appears to have a perbullar internal carotid and an extratympanic origin for the proximal stapedial as in the brown rat, and *Reithroparamys* has only a proximal stapedial artery and no internal carotid entering the cranial cavity.

Veins.—In the brown rat, most of the venous drainage from the transverse sinus is into the postglenoid vein, which

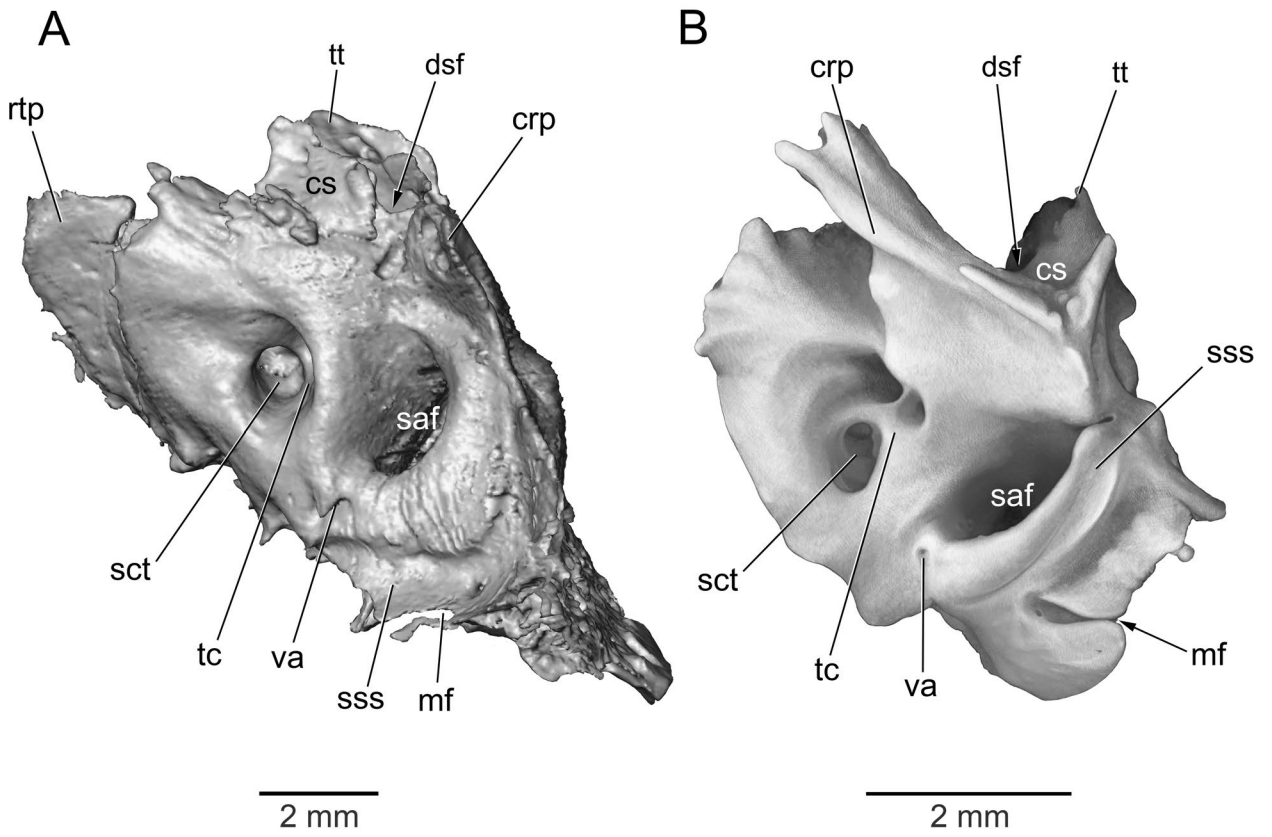

Fig. 24.—Right petrosals in dorsal view, anterior to the top of the page. **A,** *Paramys delicatus*, AMNH 12506, isosurface rendered from CT data; **B,** *Rattus norvegicus*, CM teaching collection (see Fig. 9A). Abbreviations: **crp,** crista petrosa; **cs,** cerebral surface; **dsf,** distal stapedial artery foramen; **mf,** mastoid foramen; **rtp,** rostral tympanic process; **saf,** subarcuate fossa; **sct,** spiral cribriform tract; **sss,** sigmoid sinus sulcus; **tc,** transverse crest; **tt,** tegmen tympani; **va,** vestibular aqueduct.

exits the cranium via a gap between the squamosal and tegmen tympani continuous anteriorly with the piriform fenestra (Figs. 2, 13C). The smaller sigmoid sinus supplies an occipital emissary vein out the mastoid foramen, and then most of its outflow leaves the cranium via the foramen magnum (Fig. 13C). The inferior petrosal sinus runs between the pars cochlearis and basioccipital in an incomplete canal that is open endocranially; dorsal to the jugular foramen it joins a small vein from the sigmoid sinus to form the internal jugular vein. Lastly, a small superior petrosal sinus occupies a variably present sulcus on the lateral aspect of the crista petrosa.

Veins have been largely overlooked in studies on the Eocene rodents considered here. Based on the CT scans of *Paramys delicatus*, we offer some preliminary remarks. The most striking observation is that the major venous conduits in and around the petrosal are humongous, especially compared to those in the brown rat (Figs. 20-24) The transverse sinus in *Paramys delicatus* ran in a broad sulcus on the posterior aspect of the tentorial process of the parietal ("tss" in Fig. 21). At its ventral end, the transverse sinus divided into two large veins: the postglenoid vein and the sigmoid sinus. The former exited the cranium at the large postglenoid foramen in the sidewall of the squamosal ("pgf" in Figs. 20–21). A postglenoid foramen in the same position occurs in *Paramys copei* (Wood 1962: fig. 13B), *Cocomys* (Wible et al. 2005: fig. 7), *Reithroparamys* (Meng 1990: fig. 2), and probably *Exmus* (Wible et al. 2005); in fact, an exit for the postglenoid vein on the sidewall of the braincase rather than on the ventral skull base is broadly present in Glires (rodents and lagomorphs), although not, for example, in early Eocene *Rhombomylus* (Meng et al. 2003; Asher et al. 2005; Wible 2007). Peering into the postglenoid foramen from the exterior in *Paramys delicatus*, the crista petrosa and the tentorial process of the parietal are visible (Fig. 20). These two structures create a partial medial wall to a space where the postglenoid vein and posterior division of the ramus superior cross. In the floor of this space is an entrance into a short canal in the squamosal that opens on the ventral surface anterior to the tegmen tympani ("vf" in Fig. 19). We are uncertain of the contents of this canal, but suggest that it is most likely

venous as the stapedial artery does not have a comparable branch in placentals (Wible 1984, 1987).

The sigmoid sinus in *Paramys delicatus* ran in a broad sulcus first in the squamosal, but then in the pars canalicularis around the subarcuate fossa ("sss" in Fig. 21). Most of the drainage from the sigmoid sinus exited at the jugular foramen ("jf" in Fig. 21), although a small condyloid canal in the exoccipital ("coca" in Fig. 21) sent some out the foramen magnum and a small occipital emissary vein left via the mastoid foramen ("mf" in Fig. 21). The inferior petrosal sinus was also very large ("ips" in Figs. 19, 23). It ran in a canal between the basioccipital and pars cochlearis, which was floored ventrally by the tympanic process of the basioccipital and the rostral tympanic process of the petrosal, and opened on the skull base where the inferior petrosal sinus joined the sigmoid sinus ventral to the jugular foramen to form the internal jugular vein; this is in contrast to the endocranial origin of the internal jugular vein in the brown rat. There is no bony indication for the presence of the superior petrosal sinus in *Paramys delicatus*.

Summary

Comparisons between the brown rat and the Eocene fossils highlight a number of similarities, some of which have limited distribution among Placentalia and may be of phylogenetic significance. That determination is beyond the scope of this report. Similarities include: a petrosal with five points of contact for the bulla; a rostral tympanic process and an epitympanic wing of the petrosal that are continuous and support the bulla; the hiatus Fallopii on the ventral surface of the epitympanic wing; a tegmen tympani that tapers and projects anteroventrally and supports the bulla; an epitympanic recess and fossa incudis that are continuous and entirely on the tegmen tympani (without squamosal contribution); the presence of a piriform fenestra distancing the petrosal from the sphenoid; an internal acoustic meatus and subarcuate fossa of subequal size; a cochlear canaliculus recessed from the jugular foramen; a proximal stapedial artery groove on the promontorium; a distal stapedial artery foramen on the endocranial surface of the petrosal; a single mastoid foramen; an exit for the postglenoid vein on the lateral braincase wall; a chordaforsatz on the ectotympanic; and a malleus with a dorsoventrally compressed head, elongate neck, and well-developed osseous lamina.

Our comparisons also highlight a number of differences between the brown rat and the Eocene fossils, which future studies may also discover are phylogenetically significant. Differences include: a petrosal more loosely held to the basicranium in the brown rat; a tegmen tympani and epitympanic wing that are broadly separated in the brown rat but contacting in *Cocomys*, *Paramys*, and *Sciuravis*; the much larger bullar contact on the epitympanic wing in the brown rat; an epitympanic recess without a confining lateral wall in the brown rat and with such a wall present in *Cocomys* and *Paramys*; an internal carotid artery with a transpromontorial course in *Cocomys*, *Paramys*, and *Sciuravus* and a perbullar course in the brown rat and probably *Exmus*; an open facial sulcus in *Cocomys*, *Paramys*, and *Sciuravis* and a closed facial canal that includes the distal stapedial artery in the brown rat; a caudal tympanic process of the petrosal that is absent in *Cocomys*, *Paramys*, and *Sciuravis* and present in three parts in the brown rat; a cochlear fossula in the brown rat but absent in *Cocomys* and *Paramys*; an internal acoustic meatus that is deep in *Paramys* and shallow in the brown rat; a crista petrosa only on the pars canalicularis in *Paramys* but also on the pars cochlearis in the brown rat; a cerebral surface on the petrosal that is tiny in *Paramys* and extensive in the brown rat; a tentorial process of the parietal in *Paramys*; the very large size of the venous sinuses on petrosal in *Paramys*; a primary exit for the sigmoid sinus via the jugular foramen in *Paramys* and via the foramen magnum in the brown rat; an inferior petrosal sinus enclosed in a canal in *Paramys* and open endocranially in the brown rat; a condyloid canal in *Paramys* and absent in the brown rat; an orbitotemporal groove in *Paramys* and absent in the brown rat; multiple foramina for rami temporales in the Eocene sample but only one in the brown rat; and an orbicular apophysis of the malleus absent in *Exmus* and present, though small, in the brown rat.

ACKNOWLEDGMENTS

Our foremost debt of gratitude is to Paul Bowden, scientific illustrator in the Section of Mammals, Carnegie Museum of Natural History; it is hard to imagine writing about such complex anatomy without his wonderful illustrations. We also thank the late Dr. Guy Musser, Curator Emeritus of the American Museum of Natural History, whose extensive knowledge of rats helped confirm the identity of the specimen in the Teaching Collection of the Section of Mammals that was so instrumental to this study. The senior author met Guy ages ago in New York and greatly appreciated his interest and collegiality over the years. We also acknowledge Digital Morphology, a National Science Foundation funded digital library at the University of Texas at Austin, the source of the *Rattus norvegicus* CT scan data used here. We are grateful to Dr. Ornella Bertrand, University of Edinburgh, and Ruth O'Leary, American Museum of Natural History, for assistance in accessing the CT scans of *Paramys delicatus*. Funding for this project is from National Science Foundation Grant DEB 1654949, and the R.K. Mellon North American Mammal Research Institute.

LITERATURE CITED

ALBUQUERQUE, A.A.S., M. ROSSATO, J.A.A. DE OLIVEIRA, AND M.A. HYPPOLITO. 2009. Understanding the anatomy of ears from guinea pigs and rats and its use in basic otologic research. Brazilian Journal of Otorhinolaryngology, 75(1):43–49.

ANTHWAL, N., L. JOSHI, AND A.S. TUCKER. 2013. Evolution of the mammalian middle ear and jaw: adaptations and novel structures. Journal of Anatomy, 222:147–160.

ASHER, R.J., J. MENG, J.R. WIBLE, M.C. MCKENNA, G.W. ROUGIER, D. DASHZEVEG, AND M.J. NOVACEK. 2005. Stem Lagomorpha and the antiquity of Glires. Science, 307(5712): 1091–1094.

BERGE, H. VAN DEN, AND J.C. VAN DER WAL. 1990. The innervation of the middle ear muscles of the rat. Journal of Anatomy, 170:99–109.

BERGE, H. VAN DEN, AND P. WIRTZ. 1989a. Detailed morphology of the tensor tympani muscle of the rat. An integrated light microscopi-

cal, morphometrical, enzyme histochemical, immunohistochemical and electron microscopical study in relation to function. Journal of Anatomy, 164:215–228.

BERGE, H. VAN DEN, AND P. WIRTZ. 1989b. Detailed morphology of the stapedius muscle of the rat. An integrated light microscopical, morphometrical, enzyme histochemical, immunohistochemical and electron microscopical study in relation to function. Journal of Anatomy, 166:157–169.

BERKENHOUT, J. 1769. Outlines of the Natural History of Great Britain and Ireland. Containing A Systematic Arrangement and Concise Description of All the Animals, Vegetables, and Fossiles which have hitherto been discovered in These Kingdoms. Volume I. Comprehending the Animal Kingdom. Elmsly, London. XIII + 233 pp.

BERTRAND, O.C., F. AMADOR-MUGHAL, AND M.T. SILCOX. 2016. Virtual endocasts of Eocene *Paramys* (Paramyinae): oldest endocranial record for Rodentia and early brain evolution in Euarchontoglires. Proceedings of the Royal Society B, 283:20152316.

BONDY, G. 1907. Beiträge zur vergleichenden Anatomie des Gehörorgans der Säuger. (Tympanicum, Membrana Shrapnelli und Chordaverlauf). Anatomische Hefte, 35(2):293–408.

BURDA, H., L. BALLAST, AND V. BRUNS. 1988. Cochlea in Old World mice and rats (Muridae). Journal of Morphology, 198(3):269–285.

BURGIN, C.J. 2017. 659. Brown rat *Rattus norvegicus*. Pp. 829–830, *in* Handbook of the Mammals of the World, Volume 7, Rodents II (D.E. Wilson, T.E. Lacher, Jr., and R.A. Mittermeier, eds.). Lynx Edicions, Barcelona.

BURGIN, C.J., J.P. COLELLA, P.L. KAHN, AND N.S. UPHAM. 2018. How many species of mammals are there? Journal of Mammalogy, 99(1):1–14.

BUTLER, H. 1967. The development of mammalian dural venous sinuses with especial reference to the post-glenoid vein. Journal of Anatomy, 102(1):33–56.

DAVIS, D.D., AND H.E. STORY. 1943. The carotid circulation in the domestic cat. Zoological Series, Field Museum of Natural History, 28(1):1–47.

DAWSON, M.R. 1961. The skull of *Sciuravus nitidus*, a middle Eocene rodent. Postilla, 53:1–13.

DE BEER, G.R. 1937. The Development of the Vertebrate Skull. Clarendon Press, Oxford. 554 pp., 143 pls.

EKDALE, E.G. 2013. Comparative anatomy of the bony labyrinth (inner ear) of placental mammals. PLoS ONE, 8(6):e66624.

EVANS, H.E. 1993. Miller's Anatomy of the Dog. W.B. Saunders, Philadelphia. 1113 pp.

FLEISCHER, G. 1973. Studien am Skelett des Gehörorgans der Säugetiere, einschließlich des Menschen. Säugetierkundliche Mitteilungen, 21:131–239.

———. 1978. Evolutionary principles of the mammalian middle ear. Advances in Anatomy, Embryology and Cell Biology, 55:1–70.

GREENE, E.C. 1935. The anatomy of the rat. Transactions of the American Philosophical Society, 27:1–370.

GUTHRIE, D.A. 1963. The carotid circulation in the Rodentia. Bulletin of the Museum of Comparative Zoology at Harvard College, 128(1):455–481.

HEBEL, R., AND M.W. STROMBERG. 1976. Anatomy of the Laboratory Rat. The Williams & Wilkins Company, Baltimore. 173 pp.

HELLSTRÖM, S., B. SALÉN, AND L.-E. STENFORS. 1982. Anatomy of the rat middle ear. Acta Anatomica, 112:346–352.

HENSON, O.W., JR. 1961. Some morphological and functional aspects of certain structures of the middle ear in bats and insectivores. University of Kansas Science Bulletin, 42(3):151–255.

HILL, J.E. 1935. The cranial foramina in rodents. Journal of Mammalogy, 16(2):121–129.

KLAAUW, C.J. VAN DER. 1923. Die Skelettstückchen in der Sehne des Musculus stapedius und nahe dem Ursprung der Chorda tympani. Zeitschrift für Anatomie und Entwicklungsgeschicte, 69:32–83.

———. 1931. The auditory bulla in some fossil mammals with a general introduction to this region of the skull. Bulletin of the American Museum of Natural History, 62(1):1–352.

LAVENDER, D., S.N. TARASKIN, AND M.J. MASON. 2011. Mass distribution and rotational inertia of "microtype" and "freely mobile" middle ear ossicles in rodents. Hearing Research, 282:97–107.

LEIDY, J. 1871. Notice of some extinct rodents. Proceedings of the Academy of Natural Sciences of Philadelphia, 1871:230–232.

LI, C.-K., J.-J. ZHENG, AND S.-Y. TING. 1989. The skull of *Cocomys lingchaensis*, an early Eocene ctenodactyloid rodent of Asia. Pp. 179–192, *in* Papers on Fossil Rodents in Honor of Albert Elmer Wood (C.C. Black and M.R. Dawson, eds.). Natural History Museum of Los Angeles County Science Series 33.

LINDSEY, J.R., AND H.J. BAKER. 2006. Historical foundations. Pp. 1–52, in The Laboratory Rat, second edition (M.A. Suckow, S.H. Weisbroth, and C.L. Franklin, eds.). Elsevier Academic Press, London.

LINNAEUS, C. 1758. Systema naturae per regna tria naturae, secundum classes, ordines, genera, species, cum characteribus, differentiis, synonymis, loci. 10th Edition, Volume 1. L. Salvii, Stockholm. 823 pp.

LOOMIS, F.B. 1907. Wasatch and Wind River rodents. American Journal of Science, 23(134): 123.

LUO, Z.-X. 2011. Developmental patterns in Mesozoic evolution of mammal ears. Annual Review of Ecology, Evolution, and Systematics, 42:355–380.

MACINTYRE, G.T. 1972. The trisulcate petrosal pattern of mammals. Pp. 275–303, *in* Evolutionary Biology, Volume 6 (T. Dobzhansky, M.K. Hecht, and W.C. Steere, eds.). Plenum Press, New York.

MACPHEE, R.D.E. 1981. Auditory regions of primates and eutherian insectivores: morphology, ontogeny, and character analysis. Contributions to Primatology, 18:1–282.

MARIVAUX, L., M. VIANEY-LIAUD, AND J.-J. JAEGER. 2004. High-level phylogeny of early Tertiary rodents: dental evidence. Zoological Journal of the Linnean Society, 142:105–134.

MARSH, O.C. 1871. Notice of some new fossil mammals and birds from the Tertiary formation of the West. American Journal of Science, 2(8):120–127.

MASON, M.J. 2001. Middle ear structures in fossorial mammals: a comparison with non-fossorial species. Journal of Zoology, 255(4):467–486.

———. 2013. Of mice, moles and guinea pigs: functional morphology of the middle ear in living mammals. Hearing Research, 301:4–18.

——— 2015. Functional morphology of rodent middle ears. Pp. 373–404, *in* Evolution of the Rodents: Advances in Phylogeny, Functional Morphology and Development (P.G. Cox and L. Hautier, eds.). Cambridge University Press, Cambridge.

MATTHEW, W.D. 1920. A new genus of rodents from the middle Eocene. Journal of Mammalogy, 1(4):168–169.

MAYNARD, R.L., AND N. DOWNES. 2019. Anatomy and Histology of the Laboratory Rat in Toxicology and Biomedical Research. Academic Press, London. 359 pp.

MCCLURE, T.D., AND G.H. DARON. 1971. The relationship of the developing inner ear, subarcuate fossa and paraflocculus in the rat. American Journal of Anatomy, 130:235–250.

MCDOWELL, S.B., JR. 1958. The Greater Antillean insectivores. Bulletin of the American Museum of Natural History, 115(3):113–214.

MENG, J. 1990. The auditory region of *Reithroparamys delicatissimus* (Mammalia, Rodentia) and its systematic implications. American Museum Novitates, 2972:1–35.

MENG, J., Y. WANG, AND C. LI. 2003. The osteology of *Rhombomylus* (Mammalia, Glires): implications for phylogeny and evolution of Glires. Bulletin of the American Museum of Natural History, 275:1–247.

NABEYA, D. 1923. The blood-vessels of the middle ear, in relation to the development of the small ear-bones and their muscles. (A preliminary report). Folia Anatomica Japonica, 1(5):243–245.

NOMINA ANATOMICA VETERINARIA, 5TH EDITION. 2005. Editorial Committee, Hannover, Columbia, Gent, Sapporo. www.wava-amav.org/Downloads/nav_2005.pdf

O'GORMAN, S. 2005. Second branchial arch lineages of the middle ear of wild-type and *Hoxa2* mutant mice. Developmental Dynamics,

234:124–131.

O'LEARY, M.A., J.I. BLOCH, J.J. FLYNN, T.J. GAUDIN, A. GIALLOMBARDO, N.P. GIANNINI, S.L. GOLDBERG, B.P. KRAATZ, Z.-X. LUO, J. MENG, X. NI, M.J. NOVACEK, F.A. PERINI, Z. RANDALL, G.W. ROUGIER, E.J. SARGIS, M.T. SILCOX, N.B. SIMMONS, M. SPAULDING, P.M. VELAZCO, M. WEKSLER, J.R. WIBLE, AND A.L. CIRRANELLO. 2013. The placental mammal ancestor and the post-KPg radiation of placentals. Science, 339(6120):662–667.

PARENT, J.-P. 1980. Recherches sur l'oreille moyenne des rongeurs actuels et fossiles. Anatomie, valeur systématique. Thèse Montpellier, Ecole Pratique des Hautes Études. Mémoires et travaux de l'Institut de Montpellier, 11:1–285.

———. 1983. Anatomie et valeur systématique de l'oreille moyenne des rongeurs actuels et fossils. Mammalia, 47:93–122.

POPESKO, P., V. RAJTOVÁ, AND J. HORÁK. 1992. A Colour Atlas of Anatomy of Small Laboratory Animals: Volume 2. Rat, Mouse and Golden Hamster. Wolfe Publishing Ltd, London. 253 pp.

ROUGIER, G.W., AND J.R. WIBLE. 2006. Major changes in the mammalian ear region and basicranium. Pp. 269–311, *in* Amniote Paleobiology: Perspectives on the Evolution of Mammals, Birds, and Reptiles (M.T. Carrano, T.J. Gaudin, R.W. Blob, and J.R. Wible, eds.). University of Chicago Press, Chicago.

SALIH, W.H.M., J.A.N. BUYTAERT, J.R.M. AERTS, P. VANDERNIEPEN, M. DIERICK, AND J.J.J. DIRCKX. 2012. Open access high-resolution 3D morphology models of cat, gerbil, rabbit, rat and human ossicular chains. Hearing Research, 284:1–5).

SEGALL, W. 1970. Morphological parallelisms of the bulla and auditory ossicles in some insectivores and marsupials. Fieldiana Zoology, 51:169–205.

SZABÓ, K. 1990. The cranial venous system in the rat: anatomical pattern and ontogenetic development. I. Basal drainage. Anatomy Embryology, 182:225–234.

———. 1995. The cranial venous system in the rat: anatomical pattern and ontogenetic development. II. Dorsal drainage. Annals of Anatomy, 177:313–322.

TANDLER, J. 1899. Zur vergleichenden Anatomie der Kopfarterien bei den Mammalia. Denkschriften Akademie der Wissenschaft, Wien, mathematisch-naturwissenschaftliche Klasse, 67:677–784.

WAHLERT, J.H. 1974. The cranial foramina of protrogomorphous rodents; an anatomical and phylogenetic study. Bulletin of the Museum of Comparative Zoology, 146(8):363–410.

———. 2000. Morphology of the auditory region in *Paramys copei* and other Eocene rodents from North America. American Museum Novitates, 3307:1–16.

WIBLE, J.R. 1984. The ontogeny and phylogeny of the mammalian cranial arterial pattern. Ph.D. dissertation, Duke University, Durham, NC, 705 pp.

———. 1986. Transformations in the extracranial course of the internal carotid artery in mammalian phylogeny. Journal of Vertebrate Paleontology, 6(4):313–325.

———. 1987. The eutherian stapedial artery: character analysis and implications for superordinal relationships. Zoological Journal of the Linnean Society, 91:107–135.

———. 1990. Late Cretaceous marsupial petrosal bones from North America and a cladistic analysis of the petrosal in therian mammals. Journal of Vertebrate Paleontology, 10(2): 183–205.

———. 2007. On the cranial osteology of the Lagomorpha. *In* Mammalian Paleontology on a Global Stage: Papers in Honor of Mary R. Dawson (K.C. Beard and Z.-X. Luo, eds.). Bulletin of Carnegie Museum of Natural History, 39: 213–234.

———. 2008. On the cranial osteology of the Hispaniolan solenodon, *Solenodon paradoxus* Brandt, 1833 (Mammalia, Lipotyphla, Solenodontidae). Annals of Carnegie Museum, 77(3): 321–402.

———. 2009. The ear region of the pen-tailed treeshrew, *Ptilocercus lowii* Gray, 1848 (Placentalia, Scandentia, Ptilocercidae). Journal of Mammalian Evolution, 16(3): 199–234.

———. 2010. Petrosal anatomy of the nine-banded armadillo, *Dasypus novemcinctus* Linnaeus, 1758 (Mammalia, Xenarthra, Dasypodidae). Annals of Carnegie Museum, 79(1):1–28.

———. 2012. The ear region of the aardvark *Orycteropus afer* Pallas, 1766 (Mammalia, Afrotheria, Tubulidentata). Annals of Carnegie Museum, 80(2): 115–146.

WIBLE, J.R., AND M. SPAULDING. 2013. On the cranial osteology of the African palm civet, *Nandinia binotata* (Gray, 1830) (Mammalia, Carnivora, Feliformia). Annals of Carnegie Museum, 82(1):1–114.

WIBLE, J.R., Y.-Q. WANG, C.-K. LI, AND M.R. DAWSON. 2005. Cranial anatomy and relationships of a new ctenodactyloid (Mammalia, Rodentia) from the early Eocene of Hubei Province, China. Annals of Carnegie Museum, 74(2): 91–150.

WOOD, A.E. 1962. The early Tertiary rodents of the family Paramyidae. Transactions of the American Philosophical Society, 52(1):3–261.

WYSOKI, J. 2008. Topographical anatomy and measurements of selected parameters of the rat temporal bone. Folia Morphologica, 67(2):111–119.

WYSS, A.R., AND J. MENG. 1996. Application of phylogenetic taxonomy to poorly resolved crown clades: a stem-modified node-based definition of Rodentia. Systematic Biology, 45(4):559–568.

YOUSSEF, E.H. 1966. The chondrocranium of the albino rat. Acta Anatomica, 64:586–617.

———. 1969. Development of the membrane bones and ossification of the chondrocranium in the albino rat. Acta Anatomica, 72:603–623.